ARCHIVIO ISTITUZIONALE DELLA RICERCA

Alma Mater Studiorum Università di Bologna
Archivio istituzionale della ricerca

Adaptive and Switching Internal Model Design: ROBUST ADAPTIVE FEEDFORWARD TECHNIQUES FOR STABLE SYSTEMS

This is the final peer-reviewed author's accepted manuscript (postprint) of the following publication:

Published Version:
Wang, Y., Gong, Y., Ji, C., Pin, G., Serrani, A., Parisini, T. (2025). Adaptive and Switching Internal Model Design: ROBUST ADAPTIVE FEEDFORWARD TECHNIQUES FOR STABLE SYSTEMS. IEEE CONTROL SYSTEMS, 45(6), 52-71 [10.1109/MCS.2025.3609674].

Availability:
This version is available at: https://hdl.handle.net/11585/1031259 since: 2025-12-16

Published:

DOI: http://doi.org/10.1109/MCS.2025.3609674

Terms of use:

Some rights reserved. The terms and conditions for the reuse of this version of the manuscript are specified in the publishing policy. For all terms of use and more information see the publisher's website.

This item was downloaded from IRIS Università di Bologna (https://cris.unibo.it/).
When citing, please refer to the published version.

(Article begins on next page)

11 September 2026

Adaptive and Switching Internal Model Design

ROBUST ADAPTIVE FEEDFORWARD TECHNIQUES FOR STABLE SYSTEMS

YANG WANG, YIZHOU GONG, CHENYANG JI, GILBERTO PIN, ANDREA SERRANI and THOMAS PARISINI

The problem of rejecting unwanted periodic disturbances or assigning a specified periodic evolution to the output of a dynamical system occupies a central role in control theory, as the presence of external periodic forcing occurs in a large number of control engineering applications. In particular, the problem of rejecting periodic or repetitive disturbances at the plant input has been addressed in the context of damping control of vibrating structures [1], active noise control [2], control of rotating mechanisms with eccentricity [3], control of hard disk drives [4], suppression of vibrations in helicopters [5], [6], and control of marine systems [7], to cite just a few application domains. From the theoretical standpoint, the two problems (tracking vs. rejection) are handled in a unifying setup, known as the output regulation problem, once the external forcing signal is modeled as the output of an autonomous dynamical system (the so-called exosystem). The resulting common formulation consists in rejecting an equivalent disturbance at the plant input, while stabilizing the plant by feedback from the regulated error.

Internal model principle

In the case of LTI systems, the general solution of the output regulation problem has been known since the seminal work of Wonham, Francis and Davison [8]–[10], and reposes upon the celebrated *internal model principle*, which states that robust regulation is achieved if and only if the controller embeds a suitable copy of the exosystem, called an internal model. The role of the internal model is that of securing that the corresponding closed-loop system has a transfer function between the exogenous input and the tracking error possessing a set of transmission zeros that includes all the eigenvalues of the exosystem. Once an in-

ternal model is added to each output channel [11] in such a way that the resulting interconnection is stabilizable, the design is completed by an output feedback controller providing robust stability of the closed loop. A remarkable feature of internal model-based control schemes is that they guarantee asymptotic decay of the error in presence of plant model uncertainties, as long as the stability of the overall feedback loop is preserved.

Summary

This work addressees the output regulation problem for linear systems that are either uncertain yet internally stable, or have been rendered internally stable through feedback, offering a perspective that is somewhat complementary to classical internal model-based methodologies. The paradigm we follow is that of *adaptive feedforward control*, signifying all those design methodologies that place a model of the signal to be tracked or rejected by a controlled system outside of the main feedback loop used for stabilization.

Adaptive feedforward

An alternative design philosophy is provided by the so-called *adaptive feedforward control* (AFC) [12], [13]. According to this approach, a stabilizing controller is designed first, and then a feedforward action is provided to offset the steady-state error arising in the stable loop (see Figure 1). The feedforward control is generally computed adaptively by means of on-line pseudo-gradient optimization. An obvious requirement is that the additional feedback path generated by the adaptation mechanism does not destroy the internal stability of the loop.

The development of AFC has progressed from requiring known disturbance frequencies and accurate plant models to addressing scenarios with unknown frequencies

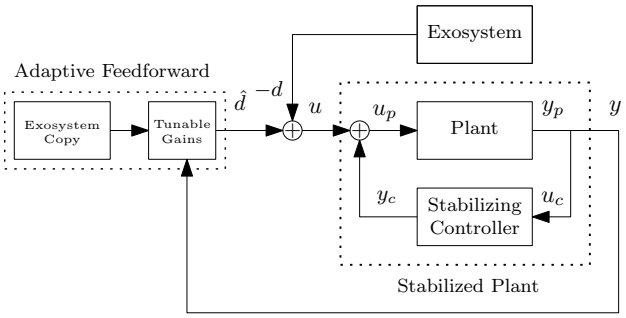

FIGURE 1 Typical setup of the AFC problem. An internal model unit is added to a compensated system outside of the main control loop to provide asymptotic tracking or a periodic reference signal or rejection of a periodic disturbance.

[14]–[16] or uncertain plant models [17]–[19]. While both AFC and classical internal model-based methods aim to achieve asymptotic disturbance rejection by embedding the disturbance dynamics, they differ in implementation. Internal model approaches typically rely on plant models and structural assumptions, while AFC separates disturbance rejection from stabilization, allowing a fully model-free design based solely on output measurements. This decoupling makes AFC particularly suited for uncertain or poorly modeled systems, thus complementing the classical theory and broadening its applicability.

The aim of this paper is to provide a somewhat unifying perspective to adaptive feedforward control that, starting from its classic setup rooted in adaptive control techniques, presents subsequent developments, cast in the framework of internal model-based control and output regulation theory, to encompass recent results that combine switching and adaptive control strategies. The guiding principle in this journey is the quest for adaptive solutions, that is, solutions that are guaranteed to hold in spite of model uncertainty. In the spirit of a tutorial exposition, we have distilled the problem to its very essence: a single-input, single-output stable (or compensated) LTI plant, subject to

a single-tone periodic disturbance with known frequency, but unknown amplitude and phase. Although this setup is certainly limited in scope, it does contain all the features that reveals the challenges encountered in the application of AFC techniques to uncertain models. The methodologies reviewed in the paper have been tested in a comparative experimental study performed on an instrumented acoustic duct. Additionally, we discuss potential extensions and provide a summary table (Table 6) of the methodologies covered.

PROBLEM FORMULATION

Output Regulation Problem

Consider the linear single-input single-output system perturbed by a single harmonic disturbance:

$$\begin{aligned} \dot{w} &= Sw, \quad w(0) = w_0 \in \mathbb{R}^2 \\ \dot{x} &= Ax + Bu + Ew, \quad x(0) = x_0 \in \mathbb{R}^n \\ y &= Hw + Cx, \quad y \in \mathbb{R} \end{aligned} \tag{1}$$

where the exosystem $\dot{w} = Sw$ generates both the disturbance $d_0 = Ew$ acting on the plant and reference signal $y_r = -Hw$ for the plant output $y_0 = Cx$. The output regulation problem is concerned with designing an output feedback law in a possibly time-varying and nonlinear form

$$\begin{aligned} \dot{\zeta} &= f_c(t, \zeta, y), \quad \zeta(0) = \zeta_0 \in \mathbb{R}^m, \\ u &= h_c(t, \zeta, y) \end{aligned} \tag{2}$$

such that the regulated output y converges to zero and all closed-loop trajectories are bounded.

Necessary and sufficient conditions for the existence of the solution of the output regulation problem were obtained by [8]–[10]:

[A1] the pair (A, B) is stabilizable;

[A2] the pair (A, C) is detectable;

[A3] the non-resonance condition rank $\begin{bmatrix} A-\lambda I & B \\ C & 0 \end{bmatrix} = n + 1$ holds for all eigenvalues λ of S.

The condition [A3] is equivalent to the existence of the unique solution pair (Γ_0, γ_0) which solves the regulator equations, also known as Francis' equations:

$$\begin{aligned} \Gamma_0 S &= A\Gamma_0 + B\gamma_0 + E, \\ C\Gamma_0 + H &= 0. \end{aligned} \tag{3}$$

Internal Model-based Approach

The classical internal model-based feedback control law takes the form of the linear system

$$\begin{aligned} \dot{\zeta} &= L_\zeta \zeta + L_y y, \\ u &= K_\zeta \zeta + K_y y, \end{aligned} \tag{4}$$

which comprises both a stabilizer and an internal model unit that generates an estimate of w. For illustrative purposes only, consider the much simpler *full-information case*, where the controller has access to the state of both the plant and exosystem models, yielding the memory-less feedback law $u = -K_1 x + K_2 w$. With the regulation equation (3) in mind, choosing K_1 such that $A - BK_1$ is Hurwitz and $K_2 = \gamma_0 + K_1 \Gamma_0$, it follows that the resulting error dynamics

$$\begin{aligned} \dot{\tilde{x}} &= (A - BK_1)\tilde{x}, \\ y &= C\tilde{x} \end{aligned}$$

are exponentially stable, where $\tilde{x} := x - \Gamma_0 w$. However, the design of the vector K_2 requires full knowledge of the system matrices A, B, C through the regulation equation. In the context of general nonlinear systems, significant effort has been made to circumvent the explicit solution of the regulator equation (3).

In internal model-based control, a classic strategy consists in first designing the internal model and then finding a stabilizer for the augmented error system. Alternatively, one may adopt a different paradigm: Under the assumption that the plant is *stable or has been pre-stabilized*, a compensator for an equivalent input disturbance is designed according to the paradigm of adaptive feedforward

control. Recent results have shown that the design of the disturbance compensator requires no prior knowledge of the plant dynamics, thus achieving a fully model-free implementation. To proceed, we let $d = \gamma_0 w$ denote the equivalent input disturbance in question. For notational convenience, however, we shall continue to denote the transformed state $\tilde{x} = x - \Gamma_0 w$ as x in the subsequent analysis. The formal problem formulation is presented in the following section.

Disturbance Rejection Problem

We consider SISO LTI models in matched disturbance form

$$\begin{aligned} \dot{x} &= Ax + B(u - d)\,, \quad x(0) = x_0 \in \mathbb{R}^n \\ y &= Cx \end{aligned} \tag{5}$$

with state $x \in \mathbb{R}^n$, control input $u \in \mathbb{R}$, disturbance input $d \in \mathbb{R}$, and regulated output $y \in \mathbb{R}$. For future use, we let

$$P(s) = C(sI - A)^{-1}B$$

denote the transfer function of (5). The premise of AFC is that the plant (5) is either a priori *internally stable*, or has been stabilized via a pre-designed controller. That is, one may interpret (5) as the interconnection $u_p = y_c + u - d$, $u_c = y_p$, and $y = y_p$ of a plant model

$$\begin{aligned} \dot{x}_p &= A_p x_p + B_p u_p\,, \quad x_p(0) = x_{p,0} \in \mathbb{R}^{n_p} \\ y_p &= C_p x_p \end{aligned} \tag{6}$$

and a stabilizing output-feedback controller

$$\begin{aligned} \dot{x}_c &= A_c x_c + B_c u_c\,, \quad x_c(0) = x_{c,0} \in \mathbb{R}^{n_c} \\ y_c &= C_c x_c + D_c u_c \end{aligned} \tag{7}$$

where, in this case,

$$A = \begin{pmatrix} A_p + B_p D_c C_p & B_p C_c \\ B_c C_p & A_c \end{pmatrix},\ B = \begin{pmatrix} B_p \\ 0 \end{pmatrix},\ C = \begin{pmatrix} C_p & 0 \end{pmatrix}.$$

Note that the matrix A is Hurwitz. For the sake of simplicity and clarity of exposition, the disturbance is given by the sinusoidal signal

$$d(t) = a\cos(\omega t + \phi), \tag{8}$$

with *known frequency* $\omega > 0$ but *unknown amplitude and phase* $a > 0$, $\phi \in [0, 2\pi)$. A state-space realization of (8) is conveniently given as the *exosystem*

$$\begin{aligned} \dot{w} &= Sw\,, \quad w(0) = w_0 \in \mathbb{R}^2 \\ d &= \Gamma w, \end{aligned} \tag{9}$$

with matrices

$$S = \begin{pmatrix} 0 & \omega \\ -\omega & 0 \end{pmatrix}, \quad \Gamma = \begin{pmatrix} 1 & 0 \end{pmatrix}$$

and initial condition $w_0 = \begin{pmatrix} w_{0,1} & w_{0,2} \end{pmatrix}^\top$ given by

$$w_{0,1} = a\cos\phi, \quad w_{0,2} = -a\sin\phi.$$

We are concerned with the design of a control signal $u(t)$ for (5) *with the least model information* of (5) such that the effect of the disturbance on the output $y(t)$ is removed, that is,

$$\lim_{t\to\infty} |y(t)| = 0, \tag{10}$$

while maintaining all internal signals bounded. Note that the system matrices A, B, C are *uncertain* and the only prior known information is the frequency of the disturbance. A formal definition of the problem at hand ensues:

Problem 1

Suppose that the plant (5) is internally stable. Find a controller of the form (2) such that the forward solutions $(x(t), \zeta(t))$, $t \geq 0$, of the closed-loop system (2), (5)-(8) driven by the exosystem (9) are bounded for all initial conditions $(x_0, \zeta_0) \in \mathbb{R}^{n+m}$ and $w_0 \in \mathbb{R}^2$, and asymptotic regulation of $y(t)$ is achieved. □

ADAPTIVE FEEDFORWARD CONTROL

Given that system (5) is internally stable, a logical strategy for the design of the controller (2) is the pursuit of a device that, using measurements of the output signal, asymptotically reconstructs and offsets the disturbance signal $d(t)$ at the input of the system, that is, yielding

$$\lim_{t\to\infty} |u(t) - d(t)| = 0.$$

This action shall be accomplished so that the inevitable feedback loop mapping y to u does not compromise the stability of the open-loop system. As a parameterized model of the disturbance is readily available, the most natural framework to cast the problem of reconstructing the disturbance $d(t)$ is that of on-line estimation of the disturbance parameters, which leads to adaptive control.

Known Plant Models: Gradient Method

It turns out that, if a sufficiently accurate model of system (5) is available, the design of the controller (2) is a routine matter, as a standard paradigm in adaptive control applies. To see why this is the case, write the disturbance in parameterized form as

$$d(t) = \Gamma e^{St} w_0 = \varphi(t)^\top w_0, \tag{11}$$

where

$$\varphi(t)^\top = \Gamma e^{St} = \begin{pmatrix} \cos(\omega t) & \sin(\omega t) \end{pmatrix}$$

is a *known regressor*, and $w_0 \in \mathbb{R}^2$ is a vector of *unknown parameters*. Consequently, (5) is written as

$$\begin{aligned} \dot{x} &= Ax + B(u - \varphi(t)^\top w_0) \\ y &= Cx. \end{aligned} \tag{12}$$

Note that in this setting, there is no need to explicitly model or estimate the state of the exosystem, as its effect is embedded in the regressor φ, constructed based on known frequency information. In the classical internal model-based approach, φ would typically be generated by an internal model that estimates the exosystem state. For instance, as shown in the section "Internal Model-based Approach", if $u(t) = \gamma_0 \zeta(t)$ and $\zeta(t)$ is a converging estimate of $w(t)$, then the control acts as feedforward compensation based on the estimated exosystem state. In contrast, within the AFC framework, the regressor φ acts as a proxy for the exosystem signal, leveraging the known frequency information. Also, system (12) takes the form of a time-varying (periodic) linear system. If w_0 were available, the obvious choice $u(t) = \varphi(t)^\top w_0$ would suffice to solve the design problem. As w_0 is unknown, we resort to the principle of *certainty equivalence*, and replace the unknown parameter vector with an estimate $\hat{w}_0(t)$, generated by a suitable update law (to be determined) of the form

$$\dot{\hat{w}}_0 = \varepsilon \tau(t, \hat{w}_0, y), \quad \hat{w}_0(0) \in \mathbb{R}^2,$$

where $\varepsilon > 0$ is a gain selected by the designer. Consequently, after applying the control

$$u = \varphi(t)^\top \hat{w}_0, \tag{13}$$

and writing the closed-loop system as

$$\begin{aligned} \dot{x} &= Ax + B\varphi(t)^\top \tilde{w}_0 \\ \dot{\tilde{w}}_0 &= \varepsilon \tau(t, \hat{w}_0, y) \\ y &= Cx, \end{aligned} \tag{14}$$

where $\tilde{w}_0 := \hat{w}_0 - w_0$ is the *parameter estimation error*, we look for an update law that achieves the objectives stated in Problem 1. Recalling that A is Hurwitz, we write the output of system (14) in the standard dynamic parametric model [20], [21]

$$y(t) = P(s)[u - \varphi(t)^\top w_0] + \epsilon(t),$$

where $\epsilon(t)$, arising from possibly nonzero initial conditions, decays exponentially to zero due to internal stability of $P(s)$. Using the augmented error notation (standard in the adaptive control literature)

$$e(t) = y(t) - P(s)[u] + P(s)[\varphi(t)^\top]\hat{w}_0(t),$$

minimization of the instantaneous cost function

$$J(\hat{w}_0) = \tfrac{1}{2} e(t)^2$$

yields the *gradient descent* for the update law

$$\dot{\hat{w}}_0 = -\varepsilon \frac{\partial J(\hat{w}_0)}{\partial \hat{w}_0}^\top = -\varepsilon P(s)[\varphi(t)] e. \tag{15}$$

Application of standard techniques from adaptive control [21, Theorem 4.5.2] shows that the gradient-based update law (15) enforces desirable properties for the forward trajectory of the estimated parameter vector:

Theorem 1 (Gradient-based update law)

Assume that the regressor $\varphi(\cdot)^\top$ is bounded. Then, the update law (15) with a filtered regressor guarantees that, for all $\varepsilon > 0$ and all initial conditions $x_0 \in \mathbb{R}^n$, $\hat{w}_0(0) \in \mathbb{R}^2$

(i) $\hat{w}_0(\cdot), \dot{\hat{w}}_0(\cdot), e(\cdot) \in \mathcal{L}_\infty$

(ii) $\dot{\hat{w}}_0(\cdot), e(\cdot) \in \mathcal{L}_2$

The x-dynamics in (14)

$$\dot{x} = Ax + B\varphi(t)^\top \tilde{w}_0(t)\,, \quad x(0) = x_0$$

is thus seen as an internally stable linear system driven by a bounded signal, hence $x(t)$, $t \geq 0$, is bounded as well. This yields boundedness of all closed-loop signals, as per the first requirement of Problem 1. Asymptotic convergence to zero of $y(t)$ follows from application of Barbălat's lemma [21, Lemma 3.2.6], since it can be shown that $y(\cdot)$ is uniformly continuous as well. Furthermore, due to the fact that the regressor is *persistently exciting*, the parameter estimation error $\tilde{w}_0(t)$ converges to zero exponentially fast, making the convergence of $y(t)$ exponential as well.

Foray Into Uncertainty: SPR Plant Models

The adaptive law (15) *with a filtered regressor* requires accurate knowledge of the plant transfer function[1] for its implementation, which is an ideal situation that is rarely encountered in applications. In case $P(s)$ is not known due to inevitable model uncertainty, but the system satisfies a stronger property than internal stability, similar results as those provided by Theorem 1 (that is, $e(\cdot) \in \mathcal{L}_\infty \cap \mathcal{L}_2$ replaced by $y(\cdot) \in \mathcal{L}_\infty \cap \mathcal{L}_2$) hold for the application of the *pseudo-gradient* update law

$$\dot{\hat{w}}_0 = -\varepsilon\varphi(t)y \tag{16}$$

[1]Another adaptation law requiring an accurate plant model is $\dot{\hat{w}}_0 = -\varepsilon B^\top P_x x$, where P_x is the unique positive definite solution to the Lyapunov equation $A^\top P_x + P_x A = -C^\top C$. Details are omitted, since similar results to those established in Theorem 1 are obtained.

to system (14). The additional property in question dictates that $P(s)$ be *strictly positive real* (SPR) [20], [21]. The key feature enabled by strict positive realness is the existence of a Lyapunov function for (14) yielding a dissipation inequality for which (16) becomes an obvious choice for the update law. The similar results of Theorem 1 follow from the ensuing Lyapunov-based analysis and from the fact that the regressor is always bounded. The SPR assumption, however, severely limits the domain of applicability of the AFC paradigm to models that are stable, minimum-phase, and with unitary relative degree.

On The Need For SPR-like Conditions In Adaptive Feedforward Control

As the SPR property [21, Theorem 3.5.1] implies that $\mathrm{Re}\{P(j\omega)\} > 0$ for all $\omega \in \mathbb{R}$, we are left to wonder whether the simpler condition $\mathrm{Re}\{P(j\omega)\} > 0$ at the frequency $\omega > 0$ of the periodic disturbance suffices for the pseudo-gradient law (16) to continue being effective in the more general case of internally stable models. As a matter of fact, the mere knowledge of $\mathrm{sign}(\mathrm{Re}\{P(j\omega)\})$ or $\mathrm{sign}(\mathrm{Im}\{P(j\omega)\})$ has been shown to provide sufficient information for the design of update laws that resemble the pseudo-gradient law (16). The price to pay, however, is that closed-loop stability and regulation can only be guaranteed for sufficiently small values of the adaptation gain $\varepsilon > 0$. This is unsurprising to a large extent. In absence of specific stability properties to be exploited in the design, we have a keen interest in ensuring that the loop gain of the closed-loop system be sufficiently small to allow the application of a suitable form of the ubiquitous small-gain theorem. From an "adaptive control perspective", it is intuitive that a sufficiently slow adaptation should be performed to maintain closed-loop stability, while the parameter estimates are tuned along the appropriate direction within the parameter space. Knowledge of the sign

of either the real or imaginary part of the plant transfer function enables this "appropriate direction" to be established by the update law. For lack of better terminology, we refer to the assumption that either $\text{sign}(\text{Re}\{P(j\omega)\})$ or $\text{sign}(\text{Im}\{P(j\omega)\})$ are known as to an *SPR-like* condition.

The second drawback of the design of update laws under SPR-like conditions is that the analysis becomes significantly more complex, even in the simplest setup considered in this paper. For historical and pedagogical reasons on one hand, and to remain true to the spirit of the internal model principle of our founding fathers, we present here *a development of AFC [12], [18]* that exploits averaging methods and small-gain analysis, all within a state-space formulation. We begin with Bodson's time-varying formulation (18), and in the subsequent section, reinterpret the time-invariant formulation by Marino and Tomei (31), establishing the equivalence between these two perspectives.

To this end, we begin to notice that the control input (13) and the update law (16) can be rewritten as

$$u = \Gamma \mathrm{e}^{St}\hat{w}_0, \quad \dot{\hat{w}}_0 = -\varepsilon \mathrm{e}^{-St}\Gamma^\top y, \tag{17}$$

respectively. The fixed vector $\Gamma^\top$ in the update law (17) is suitable for SPR plant models. For uncertain systems that do not satisfy the SPR assumption, we introduce a free design parameter $G \in \mathbb{R}^2$ in place of $\Gamma^\top$ providing additional degrees of freedom to the design of the update law. This modification in (17) leads to

$$u = \Gamma \mathrm{e}^{St}\hat{w}_0, \quad \dot{\hat{w}}_0 = -\varepsilon \mathrm{e}^{-St} G y, \tag{18}$$

which yields the closed-loop system

$$\begin{aligned} \dot{x} &= Ax + B\Gamma \mathrm{e}^{St}\tilde{w}_0 \\ \dot{\tilde{w}}_0 &= -\varepsilon \mathrm{e}^{-St} G y \\ y &= Cx. \end{aligned} \tag{19}$$

If $\varepsilon = 0$ (which implies that $\tilde{w}_0(t) = \text{const} = \tilde{w}_0$), the closed-loop system admits a unique steady-state response $x_{\text{ss}}(t)$, $t \geq 0$. We show in the sidebar "The Steady-state Response to a Sinusoidal Signal" that, indeed,

$$x_{\text{ss}}(t) = \Pi \mathrm{e}^{St}\tilde{w}_0, \tag{20}$$

where $\Pi \in \mathbb{R}^{n\times 2}$ is the unique solution of the Sylvester equation

$$\Pi S = A\Pi + B\Gamma. \tag{21}$$

When $\varepsilon > 0$, hence $\tilde{w}_0(t)$ is no longer constant, we regard $x_{\text{ss}}(t)$ as a "quasi steady-state" solution, taking comfort from the fact that we expect ε to be "sufficiently small", hence $\tilde{w}_0(t)$ to evolve on a slower time scale than $x(t)$. Consequently, we define the change of variables

$$\tilde{x} = x - \Pi \mathrm{e}^{St}\tilde{w}_0$$

that describes the transient response of the system towards the "quasi steady-state" solution. Expressing the closed-loop system in the coordinates $(\tilde{x}, \tilde{w}_0)$ and using (21) yield

$$\begin{aligned} \dot{\tilde{x}} &= A\tilde{x} + (A\Pi + B\Gamma - \Pi S)\mathrm{e}^{St}\tilde{w}_0 - \Pi \mathrm{e}^{St}\dot{\tilde{w}}_0 = A\tilde{x} - \Pi \mathrm{e}^{St}\dot{\tilde{w}}_0 \\ \dot{\tilde{w}}_0 &= -\varepsilon \mathrm{e}^{-St} G y \\ y &= C\tilde{x} + \theta^\top \mathrm{e}^{St}\tilde{w}_0 \end{aligned} \tag{22}$$

where, as shown in the sidebar "The Steady-state Response to a Sinusoidal Signal",

$$\theta^\top = C\Pi = \begin{pmatrix} \theta_1 & \theta_2 \end{pmatrix} = \begin{pmatrix} \text{Re}\{P(j\omega)\} & \text{Im}\{P(j\omega)\} \end{pmatrix}.$$

Further expanding (22) leads to the periodic system

$$\begin{aligned} \dot{\tilde{x}} &= (A + \varepsilon \Pi G C)\,\tilde{x} + \varepsilon \Pi G \theta^\top \mathrm{e}^{St}\tilde{w}_0 \\ \dot{\tilde{w}}_0 &= -\varepsilon \Phi(t)\tilde{w}_0 - \varepsilon \mathrm{e}^{-St} G C \tilde{x}, \end{aligned} \tag{23}$$

where $\Phi(t) = \mathrm{e}^{-St} G \theta^\top \mathrm{e}^{St}$. The system

$$\dot{\tilde{w}}_0 = -\varepsilon \Phi(t)\tilde{w}_0$$

is in a form amenable to application of averaging analysis [22]–[24]. In particular, let $T = 2\pi/\omega$ be the period of the disturbance, and let

$$\Phi_{\text{avg}} = \frac{1}{T}\int_0^T \Phi(\tau)\mathrm{d}\tau$$

be the average of $\Phi(t)$ over the period. Then, following [22] and [25, Section 10.4], there exist a constant $\varepsilon^* > 0$ and a T-periodic matrix $P_\Phi(t,\varepsilon) \in \mathbb{R}^{2\times 2}$, such that:

(i) $P_\Phi(t,\varepsilon)$ is nonsingular for all $\varepsilon \in (0,\varepsilon^*)$ and $t \geq 0$, and satisfy, for some $\kappa_1, \kappa_2 > 0$,

$$\|P_\Phi(t,\varepsilon)\| \leq \kappa_1, \quad \|P_\Phi(t,\varepsilon)^{-1}\| \leq \kappa_2;$$

(ii) For all $t \geq 0$ and all $\varepsilon \in (0,\varepsilon^*]$

$$P_\Phi(t,\varepsilon)^{-1}\Phi(t)P_\Phi(t,\varepsilon) + \dot{P}_\Phi(t,\varepsilon)^{-1} = \Phi_{\text{avg}} + \varepsilon Q(t,\varepsilon),$$

where $\|Q(t,\varepsilon)\| \leq \kappa_3$ for some $\kappa_3 > 0$.

Consequently, the change of coordinates

$$\zeta = P_\Phi(t,\varepsilon)^{-1}\tilde{w}_0$$

transforms system (23) into

$$\begin{aligned}\dot{\tilde{x}} &= (A + \varepsilon\Pi GC)\,\tilde{x} + \varepsilon\Delta_1(t,\varepsilon)\zeta \\ \dot{\zeta} &= -\varepsilon\Phi_{\text{avg}}\zeta + \varepsilon^2 Q(t,\varepsilon)\zeta + \varepsilon\Delta_2(t,\varepsilon)\tilde{x},\end{aligned} \tag{24}$$

where

$$\Delta_1(t,\varepsilon) = \Pi G\theta^\top \mathrm{e}^{St}P_\Phi(t,\varepsilon),\ \Delta_2(t,\varepsilon) = -P_\Phi(t,\varepsilon)^{-1}\mathrm{e}^{-St}GC$$

are bounded perturbations for all $\varepsilon \in (0,\varepsilon^*]$.

To analyze the stability of system (24), we proceed by choosing the matrix G appropriately and selecting a sufficiently small value of ε to enforce a small-gain interconnection between the $\tilde{x}$- and the ζ-subsystems. To this end, letting $G = (g_1 \ \ g_2)^\top$, the matrix Φ_{avg} is computed as

$$\Phi_{\text{avg}} = \frac{g_1}{2}\begin{pmatrix}\theta_1 & \theta_2 \\ -\theta_2 & \theta_1\end{pmatrix} + \frac{g_2}{2}\begin{pmatrix}\theta_2 & -\theta_1 \\ \theta_1 & \theta_2\end{pmatrix},$$

which yields

$$\Phi_{\text{avg}} + \Phi_{\text{avg}}^\top = (g_1\theta_1 + g_2\theta_2)I.$$

As a result, if $\theta_1 \neq 0$ and its sign is known, it suffices to select $g_1 = \text{sign}(\theta_1)$ and $g_2 = 0$ to render $-\varepsilon\Phi_{\text{avg}}$ a Hurwitz matrix. Conversely, if $\theta_2 \neq 0$ and its sign is known, the same outcome is obtained by selecting $g_1 = 0$ and $g_2 = \text{sign}(\theta_2)$. Once the appropriate G has been fixed, the system

$$\dot{\zeta} = -\varepsilon\left(\Phi_{\text{avg}}\zeta + \varepsilon Q(t,\varepsilon)\right)\zeta$$

becomes exponentially stable for sufficiently small values of ε within the previously established range $(0,\varepsilon^*]$. This can be easily established using the Lyapunov function candidate $V_\zeta(\zeta) = \zeta^\top\zeta$ and the bound for $Q(t,\varepsilon)$. Following [26], the same Lyapunov function can be used to show that the ζ-subsystem is finite $\mathcal{L}_2$-gain stable with respect to the input $\tilde{x}$, with linear $\mathcal{L}_2$-gain that can be bounded by a constant independent of ε. Specifically, the analysis of [26, Section 10.7] shows that, owing to the boundedness of $\Delta_2(t,\varepsilon)$, there exist $\gamma_\zeta > 0$ and $\beta_\zeta \geq 0$ such that, for all $\varepsilon > 0$ sufficiently small,

$$\|\zeta(\cdot)\|_2 \leq \gamma_\zeta\|\tilde{x}(\cdot)\|_2 + \beta_\zeta$$

where $\|\cdot\|_2$ denotes the $\mathcal{L}_2$ norm of a signal, $\|\zeta(\cdot)\|_2 = \int_0^\infty \|\zeta(\tau)\|^2 \mathrm{d}\tau$.

A similar analysis conducted using the Lyapunov function candidate $V_{\tilde{x}}(\tilde{x}) = \tilde{x}^\top P_a\tilde{x}$, where $P_a > 0$ is the unique solution of

$$A^\top P_a + P_a A = -I,$$

shows that the $\tilde{x}$-subsystem is finite gain $\mathcal{L}_2$-stable with respect to the input ζ for all sufficiently small values of $\varepsilon > 0$. As opposed to the previous case, however, this time the $\mathcal{L}_2$-gain of the $\tilde{x}$-subsystem scales with ε. As a matter of fact, the analysis shows that there exist $\gamma_{\tilde{x}} > 0$ and $\beta_{\tilde{x}} \geq 0$ such that, for all $\varepsilon > 0$ sufficiently small,

$$\|\tilde{x}(\cdot)\|_2 \leq \varepsilon\gamma_{\tilde{x}}\|\zeta(\cdot)\|_2 + \beta_{\tilde{x}}$$

As a result, the small-gain condition

$$\varepsilon\gamma_{\tilde{x}}\gamma_\zeta < 1$$

is enforced by selecting $\varepsilon > 0$ small enough. If this is the case, the closed-loop system is (globally) asymptotically stable by virtue of the small-gain theorem for finite $\mathcal{L}_2$-gain and detectable systems [26, Corollary 10.8.2]. Also, as the Lyapunov functions V_η and $V_{\tilde{x}}$ are quadratic, global exponential stability follows [25, Theorem 4.10]. This, in turn, implies boundedness of all trajectories and asymptotic regulation of $y(t)$.

The Steady-state Response to a Sinusoidal Signal

Consider the SISO linear system

$$\begin{aligned} \dot{x} &= Ax + Bu\,, \quad x(0) = x_0 \in \mathbb{R}^n \\ y &= Cx \end{aligned} \tag{S1}$$

where it is assumed that $A \in \mathbb{R}^{n\times n}$ is Hurwitz. Let the input u be generated by the linear autonomous system

$$\begin{aligned} \dot{w} &= Sw\,, \quad w(0) = w_0 \in \mathbb{R}^2 \\ u &= \Gamma w, \end{aligned} \tag{S2}$$

where

$$S = \begin{pmatrix} 0 & \omega \\ -\omega & 0 \end{pmatrix},\ \omega > 0, \quad \Gamma = \begin{pmatrix} 1 & 0 \end{pmatrix}$$

The output of *exosystem* (S2) is the sinusoidal signal

$$u(t) = \Gamma \mathrm{e}^{St} w_0 = a\cos(\omega t + \phi),$$

where

$$a = \sqrt{w_{0,1}^2 + w_{0,2}^2}, \quad \phi = -\arctan\frac{w_{0,2}}{w_{0,1}}.$$

Loosely speaking, the *steady state response* of system (S1) driven by (S2) is defined (if it exists) as the unique solution $x_{\mathrm{ss}}(t)$ that attracts all other forward solutions, that is, such that

$$\lim_{t\to\infty} \|x_{\mathrm{ss}}(t) - x(t)\| = 0, \quad \text{for all } x_0 \in \mathbb{R}^n,\ w_0 \in \mathbb{R}^2. \tag{S3}$$

Since $x_{\mathrm{ss}}(t)$ must be a solution of (S1) for arbitrary $w_0 \in \mathbb{R}^2$, it follows that

$$x_{\mathrm{ss}}(t) = \mathrm{e}^{At} x_{\mathrm{ss}}(0) + \int_0^t \mathrm{e}^{A(t-\tau)} B\Gamma \mathrm{e}^{S\tau} w_0 \mathrm{d}\tau$$

for some $x_{\mathrm{ss}}(0) \in \mathbb{R}^n$. Consequently, for any given $x_0 \in \mathbb{R}^n$

$$x_{\mathrm{ss}}(t) - x(t) = \mathrm{e}^{At}(x_{\mathrm{ss}}(0) - x_0),$$

hence $\lim_{t\to\infty} \|x_{\mathrm{ss}}(t) - x(t)\| = 0$ for all $x_0 \in \mathbb{R}^n$ and all $w_0 \in \mathbb{R}^2$ if and only if A is a Hurwitz matrix. By uniqueness of solutions of (S1) –(S2), $x_{\mathrm{ss}}(t)$ is the only solution satisfying (S3).

Following [26, Section 10.9], consider now the *Sylvester equation*

$$\Pi S = A\Pi + B\Gamma \tag{S4}$$

in the unknown $\Pi \in \mathbb{R}^{n\times 2}$. Since the spectra of A and S are disjoint, the solution Π exists and is unique. We will show that

$$x_{\mathrm{ss}}(t) = \Pi w(t) = \Pi \mathrm{e}^{St} w_0$$

for all initial conditions $w_0 \in \mathbb{R}^2$ of (S2). To this end, note that

$$\begin{aligned} \frac{\mathrm{d}}{\mathrm{d}t} x_{\mathrm{ss}}(t) &= \Pi S w(t) = A\Pi w(t) + B\Gamma w(t) \\ &= A x_{\mathrm{ss}}(t) + Bu(t), \end{aligned}$$

hence $x_{\mathrm{ss}}(t)$ is the solution of (S1) with initial condition $x_{\mathrm{ss}}(0) = \Pi w_0$. Furthermore,

$$\begin{aligned} \frac{\mathrm{d}}{\mathrm{d}t}(x_{\mathrm{ss}}(t) - x(t)) &= \Pi S w(t) - Ax(t) - B\Gamma w(t) \\ &= (\Pi S - A\Pi - B\Gamma) w(t) + A(\Pi w(t) - x(t)) \\ &= A(x_{\mathrm{ss}}(t) - x(t)) \end{aligned}$$

hence (S3) holds as well.

The steady state response in the output for (S1) is defined as

$$y_{\mathrm{ss}}(t) = C\Pi w(t), \quad w(t) = \mathrm{e}^{St} w_0.$$

It turns out that the row vector $C\Pi \in \mathbb{R}^{1\times 2}$ bears an important relation with the transfer function of (S1), $P(s) = C(sI - A)^{-1}B$. Let $v \in \mathbb{C}^2$ be defined as

$$v = \begin{pmatrix} 1 \\ j \end{pmatrix}, \quad j = \sqrt{-1}.$$

Multiplying each side of (S4) from the right by v yields

$$\begin{pmatrix} \Pi_1 & \Pi_2 \end{pmatrix} \begin{pmatrix} 0 & \omega \\ -\omega & 0 \end{pmatrix} \begin{pmatrix} 1 \\ j \end{pmatrix} = \begin{pmatrix} A\Pi_1 & A\Pi_2 \end{pmatrix} \begin{pmatrix} 1 \\ j \end{pmatrix} + B,$$

hence

$$\begin{aligned} -\omega\Pi_2 + j\omega\Pi_1 &= A\Pi_1 + jA\Pi_2 + B, \\ (j\omega I - A)(\Pi_1 + j\Pi_2) &= B, \\ \Pi_1 + j\Pi_2 &= (j\omega I - A)^{-1}B \end{aligned}$$

As a result,

$$C\Pi_1 + jC\Pi_2 = P(j\omega)$$

hence

$$C\Pi = \begin{pmatrix} \mathrm{Re}\{P(j\omega)\} & \mathrm{Im}\{P(j\omega)\} \end{pmatrix}.$$

RECONCILING AFC WITH REGULATOR THEORY

The results of the previous section states that there exists at least one element of the family of controllers

$$\begin{aligned}\dot{\hat{w}}_0 &= -\varepsilon \mathrm{e}^{-St} G_i y, \quad i \in \{1,2,3,4\} \\ u &= \Gamma \mathrm{e}^{St} \hat{w}_0,\end{aligned} \tag{29}$$

that solves Problem 1 for sufficiently small values of the gain $\varepsilon > 0$, where

$$G_1 = \begin{pmatrix} 1 \\ 0 \end{pmatrix},\ G_2 = \begin{pmatrix} 0 \\ -1 \end{pmatrix},\ G_3 = \begin{pmatrix} -1 \\ 0 \end{pmatrix},\ G_4 = \begin{pmatrix} 0 \\ 1 \end{pmatrix}. \tag{30}$$

Before proceeding further, we stop insisting on time-varying controllers, and show that (29) can be given a familiar LTI structure, which we will then cast in the framework of Wonham and Francis [9], [10]. Specifically, the Lyapunov transformation

$$\eta = \mathrm{e}^{St} \hat{w}_0$$

transform (29) into the family of LTI models

$$\begin{aligned}\dot{\eta} &= S\eta - \varepsilon G_i y, \quad i \in \{1,2,3,4\} \\ u &= \Gamma \eta,\end{aligned} \tag{31}$$

where each element is a controlled replica of the exosystem (9). The interconnection of systems (5), (9) and (31) takes the familiar form

$$\begin{aligned}\dot{w} &= Sw \\ \dot{x} &= Ax + B\Gamma(\eta - w) \\ \dot{\eta} &= S\eta - \varepsilon G_i y, \quad i \in \{1,2,3,4\}\end{aligned} \tag{32}$$

which, in the "error coordinates" $\tilde{\eta} = \eta - w$, $\tilde{x} = x - \Pi\tilde{\eta}$ (where Π is the solution of (21)) reads as

$$\begin{aligned}\dot{\tilde{x}} &= (A + \varepsilon \Pi G_i C)\tilde{x} + \varepsilon \Pi G_i \theta^\top \tilde{\eta} \\ \dot{\tilde{\eta}} &= (S - \varepsilon G_i \theta^\top)\tilde{\eta} - \varepsilon G_i C \tilde{x}, \quad i \in \{1,2,3,4\},\end{aligned} \tag{33}$$

which is the time-invariant version of (23).

Internal Model Equivalence

In case the model $\{C, A, B\}$ is the result of the feedback interconnection of the plant (6), internal model (31) and compensator (7), the overall regulator takes the form

$$\begin{aligned}\begin{pmatrix} \dot{x}_c \\ \dot{\eta} \end{pmatrix} &= \begin{pmatrix} A_c & 0 \\ 0 & S \end{pmatrix} \begin{pmatrix} x_c \\ \eta \end{pmatrix} + \begin{pmatrix} B_c \\ -\varepsilon G_i \end{pmatrix} u_r \\ y_r &= \begin{pmatrix} C_c & \Gamma \end{pmatrix} \begin{pmatrix} x_c \\ \eta \end{pmatrix} + D_c u_r,\end{aligned} \tag{34}$$

where the interconnection with the plant is defined by $u_p = y_r - d$ and $u_r = y_p$. Since the regulator equation for system (5) driven by (9), that is,

$$\begin{aligned}\Psi S &= A\Psi - B\Gamma + BY \\ C\Psi &= 0\end{aligned}$$

admits the solution $(\Psi, Y) = (0, \Gamma)$, the regulator (34) trivially obeys the internal model property

$$\begin{pmatrix} A_c & 0 \\ 0 & S \end{pmatrix} \Sigma = \Sigma S, \quad \begin{pmatrix} C_c & \Gamma \end{pmatrix} \Sigma = \Gamma$$

by virtue of $\Sigma \in \mathbb{R}^{(n_c+2)\times 2}$ given by

$$\Sigma = \begin{pmatrix} 0 \\ I \end{pmatrix}.$$

The family of controllers (31), which we now legitimately regard as internal models of the exosystem, has been originally proposed in [18]. Therein, the authors dispose altogether of the need to resort to averaging methods by employing clever elementary root-locus arguments to prove the existence of stabilizing controllers within the given family, therefore severing the ties with the classic methods of [12], [13]. In this tutorial exposition, however, we have preferred to present this development as a natural evolution of the adaptive feedforward paradigm.

REMOVING SPR-LIKE CONDITIONS

The internal models (31) are all of fixed structure, and any relation to adaptation has been removed. As a matter of fact, once an SPR-like condition hold, the choice of

a viable internal model among the given family and a suitable selection of the gain $\varepsilon > 0$ suffice to obtain regulation. It should be noted that, as the disturbance has been assumed to be persistent (that is, $a > 0$ in (8)), it has been tacitly assumed that $P(j\omega) \neq 0$ for all frequencies of interest, otherwise we would be dealing with a moot problem. Also, the solvability condition [A3] of the output regulation problem in the section "Output Regulation Problem" together with the assumption of internal stability of the plant implies that $P(j\omega) \neq 0, \forall \omega \in \mathbb{R}$ [27], [28]. As a result, $\theta \neq 0$, which implies that either $\theta_1 \neq 0$, or $\theta_2 \neq 0$, or both components of θ are nonzero. In this latter case, two out of four internal models in (31) are viable candidates. The issue becomes the knowledge of the sign(θ_1) and/or sign(θ_2), since in absence of such information, the selection of the viable internal model candidate cannot be performed. This scenario brings back the need for adaptation of the internal model units within the given class, with the goal of achieving an automatic selection of the viable candidate. In preparation for the subsequent developments, we introduce a reasonable assumption on the parameter vector θ, in order to guarantee a minimum level of a priori information that can be retrieved from the steady-state response of (5) when forced by (9).

Assumption 1

The vector θ satisfies

$$\theta \in \Theta = \{\theta \in \mathbb{R}^2 \mid r_1^2 \leq \|\theta\|^2 \leq r_2^2\} \tag{35}$$

for known constants $0 < r_1 < r_2$.

This assumption is necessary to avoid that $P(j\omega)$ vanishes as ω ranges over a set of known frequencies of interest. It is worth noticing that Assumption 1 entails a *uniform complete observability* condition (where "uniformity" is meant with respect to the uncertain parameter θ) of the stead-state response of the system. As a matter of fact, the observability Gramian $W_o(t)$ of the system

$$\dot{w} = Sw, \quad w(0) = w_0 \in \mathbb{R}^2$$

$$y_{ss} = -\theta^\top w$$

that governs the steady-state output response of (5)-(9) when $u = 0$, satisfies

$$W_o(t+T) = \tfrac{1}{2}\|\theta\|^2 I \geq \tfrac{1}{2} r_1^2, \quad \text{for all } t \geq 0.$$

Furthermore, Assumption 1 guarantees the following result, which is a consequence of compactness of the set Θ, where $\|\theta\|$ is bounded away from zero:

Lemma 1

There exists $\varepsilon^\star > 0$ such that for any $\theta \in \Theta$, the viable candidate internal models (31) yield an exponentially stable closed-loop system (33) for all $\varepsilon \in (0, \varepsilon^\star]$.

In principle, the gain $\varepsilon > 0$ of the internal model units can be selected once and for all from a sufficient a priori knowledge of the uncertain (compensated) plant model.

Switching Internal Model

The most natural approach to provide an automatic selection of a viable regulator is to endow the family of internal models (31) with a supervisor. Within the internal model paradigm, switching [29]–[31] or hybrid techniques [32]–[34] have been employed to provide adaptation with respect to unknown frequencies of the exosystem, as an alternative (quite often, a betterment) over classic continuous-time [35]–[39] or discrete-time solutions [1], [40]. Here, a supervised switching mechanism is introduced to enforce stabilizability of the internal model unit via low-gain feedback. In [41], several possibilities are presented for the design of a supervisory system generating a switching logic for the selection of the candidate internal model (pre-routed [42], hysteresis [43], and dwell-time switching [44]), all within the general paradigm of state-shared multi-controllers pioneered by Morse [42], [45]. Here, we focus

on a much streamlined version (suitable for the somewhat informal style of this contribution) of the approach presented in [46], which reposes upon the *state-norm estimator* (SNE) method of [47].

Specifically, a multi-internal model unit with state space $\mathcal{E} = \mathbb{R}^2 \times \mathbb{R}^2 \times \mathbb{R}^2 \times \mathbb{R}^2$, input space $\mathcal{Y} = \mathbb{R}$ and output space $\mathcal{U} = \mathbb{R}$ is defined as the system

$$\begin{aligned} \dot{\eta}_i(t) &= S\eta_i(t) - \varepsilon G_i y(t),\ \eta_i(0) \in \mathbb{R}^2, \quad i = 1, \ldots, 4 \\ u(t) &= \Gamma \eta_{\sigma(t)}(t), \end{aligned} \tag{38}$$

with four internal models running in parallel, and output selected according to the piecewise constant switching signal $\sigma(\cdot) : \mathbb{R}_{\geq 0} \to \{1,2,3,4\}$. The signal $\sigma(t)$ remains constant over $t \in [t_k, t_{k+1})$, and switches to a new value in the set $\{1,2,3,4\}$ at $t = t_{k+1}$, $k = 0,1,2,\ldots$. The criterion for switching $\sigma(t)$ to a new index i is determined by a comparison of the norm squared of the output $|y(t)|^2$ of the closed-loop system with a time-varying threshold $\bar{y}(t) \geq 0$ that estimates an upper bound for $|y(t)|^2$ in the case a viable internal model unit had been selected and kept for all time $t \geq t_k$ (that is, if the closed-loop system has been rendered exponentially stable). If at any time $\tau > t_k$ the condition $|y(\tau)|^2 \leq \bar{y}(\tau)$ is violated, then the current selection of the internal model unit is discarded. The counter k is incremented by one unit, t_{k+1} is set at τ, and $\sigma(t_k)$ is switched to a different member in the set $\{1,2,3,4\}$. At the same time t_{k+1}, the state-norm estimator is re-initialized. In summary, the switching scheme is given as

$$\begin{aligned} \sigma(t) &= (k + \sigma(0) - 1) \mod 4 + 1, \quad \forall t \in [t_k, t_{k+1}), \\ t_{k+1} &= \inf\{t > t_k : |y(t)|^2 > \bar{y}(t)\}, \quad t_0 = 0, \end{aligned}$$

where "mod" denotes the modulo operation (i.e., the remainder after division).

The design of the state-norm estimator is built on the basis of worst-case class-$\mathcal{KL}$ estimates derived from candidate Lyapunov functions, following the general principle detailed in the sidebar "Lyapunov-based State Norm Estimators" and the methodology developed in [47]. In particular, is shown in [46] that a state-norm estimator can be built on the basis of Lyapunov functions for the top subsystem of (32), written as

$$\dot{x} = Ax + B\Gamma\tilde{\eta},$$

and for the bottom subsystem of (33), respectively. For the x-subsystem, the existence of a suitable Lyapunov function is postulated on the basis of robust stability. For the $\tilde{\eta}$-subsystem of (33), owing to Assumption 1 and Lemma 1, one exploits the fact that, when $i = i^\star$ is the index of a viable candidate, the solution $Q(\varepsilon, \theta)$ of the Lyapunov equation

$$(S - \varepsilon G_{i^\star}\theta^\top)^\top Q(\varepsilon,\theta) + Q(\varepsilon,\theta)(S - \varepsilon G_{i^\star}\theta^\top) = -\varepsilon I,$$

satisfies

$$q_1 I \leq Q(\varepsilon,\theta) \leq q_2 I$$

for all $\varepsilon \in (0, \varepsilon^\star]$ and all $\theta \in \Theta$, where $0 < q_1 \leq q_2$ are constants that can be chosen independently of ε and θ. The technical details presented in [46] are ostensively elaborate, and will be omitted.

Multiple Model Adaptive Controller

Instead of employing a fixed estimate $G_{i^\star}$ in switching internal models, an alternative approach is presented in [19], which incorporates a continuous estimation into an auxiliary input while maintaining a fixed internal model structure. In this approach, the family of internal models (31) is first replaced by the single system

$$\begin{aligned} \dot{\eta} &= S\eta + \Gamma^\top u_a \\ u &= \Gamma\eta \end{aligned} \tag{39}$$

where u aims to cancel the disturbance $d = \Gamma w$, and u_a serves as an auxiliary input to be defined to solve Problem 1 for the resulting interconnected system. This latter is written in the familiar error coordinates $\tilde{\eta} = \eta - w$,

Lyapunov-based State Norm Estimators

Consider the LTI system

$$\begin{aligned} \dot{x} &= Ax + Bu, \quad x(0) = x_0 \in \mathcal{X}_0 \subset \mathbb{R}^n \\ y &= Cx, \end{aligned} \tag{S1}$$

with state $x \in \mathbb{R}^n$, input $u \in \mathbb{R}^m$ and output $y \in \mathbb{R}^p$, and initial condition x_0 belonging to a known compact set $\mathcal{X}_0$. We assume that the model is not accurately known, for example that (C, A, B) depend continuously upon a vector $\mu \in \mathcal{P} \subset \mathbb{R}^q$ of uncertain parameters, where $\mathcal{P}$ is a known compact set. Assume also that A is Hurwitz for all $\mu \in \mathcal{P}$ and that there exists a parameter-dependent solution $P_a(\mu) = P_a(\mu)^\top$ of the Lyapunov equation

$$A^\top P_a(\mu) + P_a(\mu) A = -I$$

and known constants $0 < p_1 \leq p_2$ such that

$$p_1 I \leq P_a(\mu) \leq p_2 I$$

for all $\mu \in \mathcal{P}$. Then, given $u(t)$, $t \geq 0$, a time-varying upper bound $\bar{y}(t)$ of $\|y(t))\|^2$ can be obtained as follows: The derivative of the Lyapunov function $V_\mu(x) = x^\top P_a(\mu) x$ along solutions of (S1) can be bounded as

$$\begin{aligned} \dot{V}_\mu(x(t)) &\leq -\|x(t)\|^2 + 2\|x(t)^\top P_a B u(t)\| \\ &\leq -\|x(t)\|^2 + \tfrac{1}{2}\|x(t)\|^2 + 2\|P_a B\|^2 \|u(t)\|^2 \\ &\leq -\tfrac{1}{2p_2} V_\mu(x(t)) + 2\|P_a B\|^2 \|u(t)\|^2, \end{aligned}$$

where the inequality $ab \leq \frac{a^2}{2} + \frac{b^2}{2}$ has been used. Letting $\kappa_1 = 2 \max_{\mu \in \mathcal{P}} \|P_a B\|^2$, one obtains

$$\dot{V}_\mu(x(t)) \leq -\tfrac{1}{2p_2} V_\mu(x(t)) + \kappa_1 \|u(t)\|^2, \quad t \geq 0.$$

By the comparison principle, the solution $\chi(t)$, $t \geq 0$ of the linear differential equation

$$\dot{\chi}(t) = -\tfrac{1}{2p_2}\chi(t) + \kappa_1 \|u(t)\|^2, \quad \chi(0) = \chi_0 \tag{S2}$$

provides an upper bound for the evolution of $V_\mu(x(t))$ along the considered trajectory of (S1), provided that $\chi_0 \geq V_\mu(x_0)$. To this end, we select

$$\chi_0 = p_2 \max_{x_0 \in \mathcal{X}_0} \|x_0\|^2 \geq p_2 \|x_0\|^2 \geq V_\mu(x_0)$$

to ensure that $\chi_0 \geq V_\mu(x_0)$ for all $x_0 \in \mathcal{X}_0$ and all $\mu \in \mathcal{P}$. Finally, from the relation $p_1 \|x\|^2 \leq V_\mu(x)$, we obtain the required upper bound as

$$\bar{y}(t) = \kappa_2 \chi(t),$$

where $\kappa_2 = \frac{1}{p_1} \max_{\mu \in \mathcal{P}} \|C\|^2$.

$\tilde{x} = x - \Pi\tilde{\eta}$ as

$$\begin{aligned} \dot{\tilde{x}} &= A\tilde{x} - \Pi\Gamma^\top u_a \\ \dot{\tilde{\eta}} &= S\tilde{\eta} + \Gamma^\top u_a \\ y &= C\tilde{x} + \theta^\top \tilde{\eta}. \end{aligned} \tag{40}$$

In this setup, an additional output-feedback controller of the form

$$\begin{aligned} \dot{\xi} &= f_a(\xi, y), \quad \xi(0) = \xi_0 \in \mathcal{X} \subset \mathbb{R}^m \\ u_a &= h_a(\xi, y) \end{aligned} \tag{41}$$

must be designed such that trajectories of the closed-loop system (40)-(41) originating from all initial conditions $\tilde{x}(0) \in \mathbb{R}^n$, $\tilde{\eta}(0) \in \mathbb{R}^2$ and $\xi_0 \in \mathcal{X}$, where $\mathcal{X} \subset \mathbb{R}^m$ is a set to be determined, are bounded and satisfy $\lim_{t\to\infty} y(t) = 0$.

To design the stabilizer (41), system (40) is regarded as the interconnection of an *auxiliary system*

$$\begin{aligned} \dot{\tilde{\eta}} &= S\tilde{\eta} + \Gamma^\top u_a \\ y_a &= \theta^\top \tilde{\eta} \end{aligned} \tag{42}$$

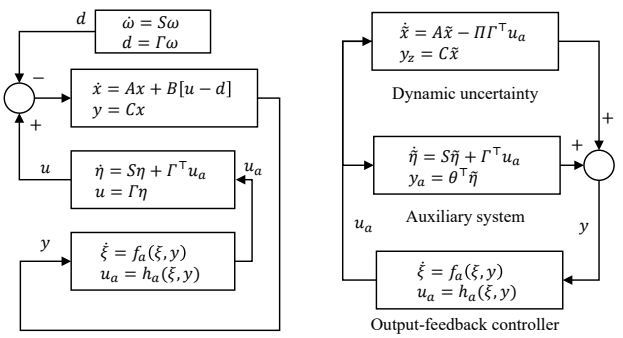

FIGURE 2 The original closed-loop system (left) can be seen as the interconnection of a dynamic uncertainty, an auxiliary system and a dynamic controller (right). Figure taken from [19], © IEEE. Reprinted with permission.

given by the $\tilde{\eta}$-dynamics, and a *dynamic perturbation*, given by the $\tilde{x}$-dynamics, as seen in Fig. 2. The idea is to design an adaptive controller for u_a focusing on the auxiliary system, and prove that stability and regulation are maintained in the presence of the dynamic perturbation induced by the plant, for a suitable selection of the gains of the controller (41).

To this end, start from the realization of the auxiliary system (42) with the coordinate change $\zeta_o = M_o^{-1}\tilde{\eta}$, where $M_o = \frac{1}{\|\theta\|^2}\begin{pmatrix}\theta_1 & -\theta_2\\ \theta_2 & \theta_1\end{pmatrix}$. An observer form is then obtained

$$\begin{aligned}\dot{\zeta}_o &= S\zeta_o + \vartheta\, u_a\\ y_a &= \Gamma\zeta_o,\end{aligned} \tag{43}$$

where

$$\vartheta = (\theta_1 \quad -\theta_2)^\top \tag{44}$$

is a reparameterization of θ, still satisfying $\vartheta \in \Theta$. For (43), we design the *adaptive observer*

$$\begin{aligned}\dot{\hat{\zeta}}_o &= S\hat{\zeta}_o + \hat{\vartheta}(t)u_a - \varepsilon\,\Gamma^\top(\hat{y}_a - y)\\ \hat{y}_a &= \Gamma\hat{\zeta}_o\end{aligned} \tag{45}$$

where $\hat{\vartheta}(t) \in \mathbb{R}^2$ is the estimate of ϑ. The dynamics of the observer error $\tilde{\zeta}_o := \hat{\zeta}_o - \zeta_o$ reads as

$$\begin{aligned}\dot{\tilde{\zeta}}_o &= F_\varepsilon\,\tilde{\zeta}_o + \tilde{\vartheta}(t)u_a + \varepsilon\,\Gamma^\top C\tilde{x}\\ \tilde{y} &= \Gamma\tilde{\zeta}_o - C\tilde{x}\end{aligned} \tag{46}$$

where $\tilde{\vartheta}(t) = \hat{\vartheta}(t) - \vartheta$ is the estimation error, $\tilde{y} = \hat{y}_a - y$. Note that $\tilde{y}(t)$ is a signal available for processing, whereas $y_a(t)$ is not. Also,

$$\tilde{y} = \Gamma\hat{\zeta}_o - C\tilde{x} - \theta^\top\tilde{\eta} = \Gamma\hat{\zeta}_o - C\tilde{x} - \Gamma\zeta_o = \Gamma\tilde{\zeta}_o - C\tilde{x}.$$

It is reassuring that the matrix

$$F_\varepsilon := S - \varepsilon\,\Gamma^\top\Gamma$$

is Hurwitz for all $\varepsilon > 0$, on account of the fact that S is skew-symmetric and (Γ, S) is an observable pair. The design of the controller for the auxiliary system is then performed in the observer space. Essentially, instead of working in the usual coordinate system "plant/ observer error" $(\zeta_o, \tilde{\zeta}_o)$, we choose to work in the "observer/ observer error" coordinates $(\hat{\zeta}_o, \tilde{\zeta}_o)$. The two representations are equivalent, but using the latter we have the advantage of being able to apply feedback from the state of the observer. As a matter of fact, we choose the certainty-equivalence control

$$u_a = -\varepsilon\,\hat{\vartheta}(t)^\top\hat{\zeta}_o \tag{47}$$

which yields, for the compensated observer dynamics,

$$\dot{\hat{\zeta}}_o = \left(S - \varepsilon\,\hat{\vartheta}(t)\hat{\vartheta}(t)^\top\right)\hat{\zeta}_o - \varepsilon\,\Gamma^\top(\hat{y}_a - y)\,. \tag{48}$$

The structure of the time-varying matrix $S - \varepsilon\,\hat{\vartheta}(t)\hat{\vartheta}(t)^\top$ in (48) is also appealing: When $\hat{\vartheta}(t) = \vartheta$, the matrix in question is Hurwitz for all $\varepsilon > 0$, as the pair $(\vartheta^\top, S)$ is observable by virtue of Assumption 1.

At this point, it is worth assembling the overall closed-loop system

$$\begin{aligned}\dot{\tilde{x}} &= A\tilde{x} + \varepsilon\Pi\Gamma^\top\hat{\vartheta}(t)^\top\hat{\zeta}_o\\ \dot{\hat{\zeta}}_o &= S\hat{\zeta}_o - \varepsilon\hat{\vartheta}(t)\hat{\vartheta}(t)^\top\hat{\zeta}_o - \varepsilon\,\Gamma^\top\Gamma\tilde{\zeta}_o + \varepsilon\,\Gamma^\top C\tilde{x}\\ \dot{\tilde{\zeta}}_o &= F_\varepsilon\,\tilde{\zeta}_o - \varepsilon\tilde{\vartheta}(t)\hat{\vartheta}(t)^\top\hat{\zeta}_o + \varepsilon\,\Gamma^\top C\tilde{x}\end{aligned} \tag{49}$$

which has the structure of a linear time-varying system (recall that $\hat{\vartheta}(t)$ has not been defined yet.) The following result, proved in [19], is key:

Theorem 2

Assume that the signal $\hat{\vartheta}(\cdot) : \mathbb{R}_{\geq 0} \to \mathbb{R}^2$ is continuously differentiable and satisfies the following properties:

(i) $\hat{\vartheta}(t) \in \Theta$ for all $t \geq 0$;

(ii) There exists a constant $\rho > 0$ such that $\|\dot{\hat{\vartheta}}(t)\| \leq \varepsilon^2 \rho$ for all $t \geq 0$;

(iii) The signal $z(t) = \xi(t)^\top \tilde{\vartheta}(t)$, $t \geq 0$, is square-integrable, where ξ is the state of the filter

$$\dot{\xi} = F_\varepsilon^\top \xi + \Gamma^\top u_a, \quad \xi(0) = 0.$$

Then, there exists $\varepsilon^\star > 0$ such that for all $\varepsilon \in (0, \varepsilon^\star]$ the trajectories of the closed-loop system (49) are bounded and asymptotic regulation of $y(t)$ is achieved.

Essentially, Theorem 2 lists the properties that an update law for $\hat{\vartheta}(t)$ must enforce on the trajectories of the parameter estimate for a successful design. Let us start from the bottom: Property (iii) is a technical result that arises from the application of the *swapping lemma* [20], [21] to system (46); we shall not dwell on it much further, except for mentioning that the state of the filter generates the regressor to be employed in the update law. Property (ii) can be enforced by adopting normalized update laws. Finally, Property (i) is the most critical from a design perspective, as the set Θ is not convex. This is a challenge, because adaptive laws usually require convex parameter sets to guarantee convergence. For this reason, we are bound to consider a convex cover $\bar{\Theta} \supset \Theta$ comprised of the union of three convex sets

$$\bar{\Theta} = \bigcup_{i=1,2,3} \Theta_i,$$

as shown in Figure 3. We then resort to the paradigm of multiple-model adaptive control approach [48]–[52] where three candidate estimators run in parallel, and a supervisor

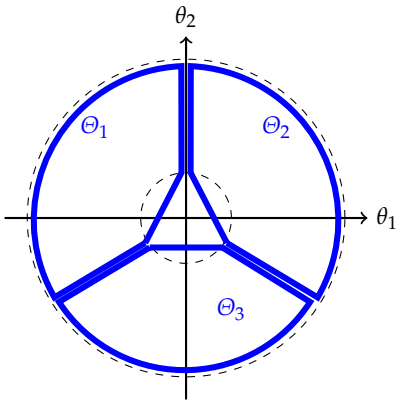

FIGURE 3 Finite covering of the non-convex parameter set Θ. Three convex sets are used, Θ_i $i = 1, 2, 3$. Three separate parameter estimates are employed, each constrained on Θ_i by means of projection. Figure taken from [19], © IEEE. Reprinted with permission.

selects the best-performing one based on a performance criterion. Since each candidate estimator, denoted by $\hat{\vartheta}^i(t)$ is projected on the corresponding set Θ_i, this strategy effectively avoid the issues caused by the non-convexity of Θ. The ensuing multi-controller is comprised of three modules: a switching controller, a multiple-model estimator, and a hysteresis-based switching logic. The three modules are presented in details in the sidebar "Multiple-Model Adaptive Controller". Using the arguments in [43], it can be shown that on each closed interval of time $[0, T]$, only a finite number of switchings may occur, therefore the Zeno behavior (infinitely fast switching) is avoided. Furthermore, there exists $\varepsilon^\star > 0$ and a finite time $T_s > 0$ such that for all $\varepsilon \in (0, \varepsilon^\star]$

$$\sigma(t) = \sigma(T_s), \quad \forall\, t \in [T_s, +\infty)$$

that is, the switchings stop at most in T_s units of time. Finally, $\sigma(T_s)$ corresponds to the index of a stabilizing controller, hence regulation is achieved.

Multiple-Model Adaptive Controller

The architecture of the adaptive multi-controller for the internal model unit presented in [19], shown in Figure S1, is comprised of three modules: A switching controller, a multiple-model estimator, and a hysteresis-based switching logic. In contrast to the switching internal model approach described in the section "Switching Internal Model", the key innovation in [19] lies in embedding the frequency response estimation directly into the auxiliary input u_a, while maintaining a fixed internal model structure. A multiple-model estimator is introduced to address the non-convexity of the set Θ, and the switching logic selects the best candidate based on the estimation error performance.

Switching Controller

The single observer-based adaptive controller (45)-(47) is replaced by three controllers of the form

$$\begin{aligned}\dot{\hat{\zeta}}_o^i &= S\hat{\zeta}_o^i + \hat{\vartheta}^i u_a^i - \varepsilon\,\Gamma^\top(\hat{y}_a^i - y)\,, \quad \hat{\zeta}_o^i \in \mathbb{R}^2\\ \hat{y}_a^i &= \Gamma\hat{\zeta}_o^i \\ u_a^i &= -\varepsilon\hat{\vartheta}^{i\top}\hat{\zeta}_o^i\,, \qquad i \in \{1,2,3\}.\end{aligned} \tag{S1}$$

running in parallel. Each single controller in (S1) depends on its own parameter estimate $\hat{\vartheta}^i$. For a piecewise constant switching signal $\sigma(\cdot) : \mathbb{R}_{\geq 0} \to \{1,2,3\}$, $\sigma(t)$ determines the output of the active controller at time t that drives the internal model unit

$$\begin{aligned}\dot{\eta}(t) &= S\eta(t) + \Gamma^\top u_a^{\sigma(t)}(t)\\ u(t) &= \Gamma\eta(t).\end{aligned}$$

Multiple-model Estimator

Each parameter estimate $\hat{\vartheta}^i(t)$, $i = 1,2,3$, constrained to evolve on the convex set Θ_i, is generated by the following update laws, sharing the common regressor $\xi(t)$:

$$\begin{aligned}\dot{\xi}(t) &= (S - \varepsilon\Gamma^\top\Gamma)^\top\xi(t) + \Gamma^\top u_a^{\sigma(t)}(t), \quad \xi(0) = 0\\ \dot{\hat{\vartheta}}^i(t) &= \mathrm{Proj}_{\Theta_i}\left\{\tau(\xi(t),\tilde{y}^i(t))\right\}, \quad \hat{\vartheta}^i(0) \in \mathrm{int}\,\Theta_i\\ \tilde{y}^i(t) &= \Gamma\hat{\zeta}_o^i(t) - y(t), \quad i \in \{1,2,3\}\end{aligned} \tag{S2}$$

where

$$\tau(\xi(t),\tilde{y}^i(t)) = -\frac{\rho\varepsilon^2\xi(t)\tilde{y}^i(t)}{1+m_i^2(t)}, \quad \rho > 0$$

is a normalized gradient-based update law,

$$m_i^2(t) := 1 + \|\xi(t)\|^2 + |\Gamma\hat{\zeta}_o^i(t) - y(t)|^2 \in \mathbb{R}$$

is a normalization signal, and $\mathrm{Proj}_{\Theta_i}\{\cdot\}$ is the standard projection on Θ_i.

Hysteresis-based Switching Logic

For each estimator/controller pair, a performance functional is designed as

$$J^i(t) = \beta\int_0^t \tilde{y}^i(\tau)^2 d\tau\,, \quad i \in \{1,2,3\} \tag{S3}$$

Let the time sequence $\{T_m\}_{m=1}^M$, denote the times at which the switching takes place; note that $T_0 = 0$ and that $M \leq \infty$. The switching logic is formally stated as

$$\sigma(T_m) := \underset{i\in\{1,2,3\}}{\arg\min}\{J_h^i(T_m)\}, \tag{S4}$$

where

$$J_h^i(T_m) := \begin{cases} J^i(T_m) & \text{if } i = \sigma(T_{m-1}) \\ J^i(T_m) + h & \text{if } i \neq \sigma(T_{m-1}) \end{cases} \qquad \forall\, i \in \{1,2,3\}$$

and $h > 0$ is the hysteresis constant. Note that $\sigma(t) = \sigma(T_m)$ in any time interval $[T_m, T_{m+1})$, $m \in \{0,1,2,\ldots\}$. The switching scheme consists in continuously monitoring the performance index $J_h^i(t)$, $i \in \{1,2,3\}$.

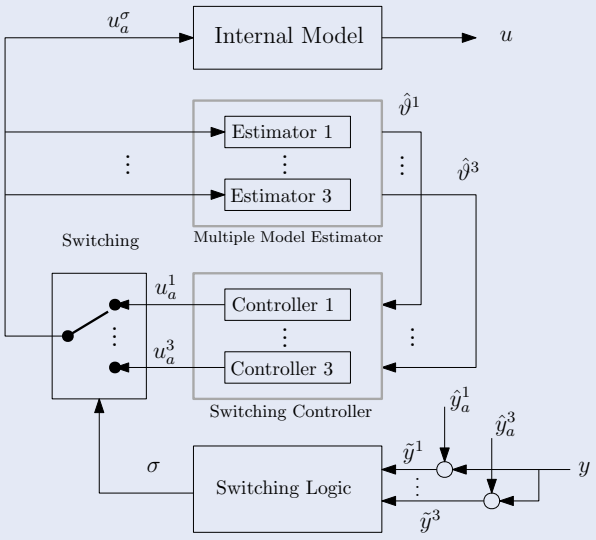

FIGURE S1 Block diagram of the multiple-model based adaptive controller for the internal model unit.

Auxiliary Estimator-based Switching Controller

The multi-controller presented in the previous sections suffers from the curse of dimensionality when we attempt at extending the methodology to the multi-frequency scenario, that is, when the disturbance

$$d(t) = \sum_{\ell=1}^{M} a_\ell \cos(\omega_\ell t + \phi_\ell), \tag{54}$$

comprises M periodic signals of *known distinct* frequency $\omega_\ell > 0$ and *uncertain* parameters $a_\ell > 0$, $\phi_\ell \in [0, 2\pi)$. If this is the case, the architecture detailed in the sidebar "Adaptive Multi-Controller" employs 3^M controller/estimator modules, each with $4M$ states. As a matter of fact, we must consider all possible combinations of estimates $\hat{\vartheta}_\ell^i$, belonging to each one of the three sets Θ_i, $i = 1, 2, 3$, for each frequency ω_ℓ, $\ell = 1, 2, \ldots, M$.

The alternative approach proposed in [53] (still presented here for a single-frequency disturbance) reduces drastically the dimension of the overall multi-controller. The point of departure is the definition of a large number of *distinct constant estimates* $\hat{\vartheta}_i$, $i \in \mathcal{I} = \{1, 2, \ldots, N\}$ of the unknown parameter ϑ. The underlying assumption is that, for any $\vartheta \in \Theta$, there exists $i \in \mathcal{N}$ such that $\hat{\vartheta}_i$ is "sufficiently close" to the true parameter vector. The selection of the actual parameter estimate $\hat{\vartheta}_i$ to be employed in the controller is performed by a hysteresis-based supervisor, which uses a single continuous time-varying estimates $\psi(t) \in \mathbb{R}^2$ of ϑ. The major advantage of this approach is that $\psi(t)$ does not need to be constrained within Θ, but only within the closed ball

$$\Omega_2 = \{\|\theta\|^2 \leq r_2^2\} \supset \Theta$$

thus avoiding the need for a multiple model estimator. The estimate $\psi(t)$ is thus allowed to transit through the ball

$$\Omega_1 = \{\|\theta\|^2 \leq r_1^2\}$$

whose boundary defines the inner boundary of Θ. The supervisor employs N performance indexes $\pi_i(t)$, defined as the distance between the continuous-time estimate $\psi(t)$ and each constant estimate $\hat{\vartheta}_i$

$$\pi_i(t) = \|\psi(t) - \hat{\vartheta}_i\|, \quad i \in \mathcal{I}. \tag{55}$$

The rationale behind this choice is simple: as $\psi(t)$ approaches a neighborhood of ϑ, the estimate $\hat{\vartheta}_i$ with the smallest $\pi_i(t)$ is likely to be the viable one. This reasoning is valid as long as $\psi(t) \in \Theta$. When $\psi(t)$ is within the interior of Ω_1, however, the continuous-time estimate may be too far from a viable candidate parameter. Therefore, the monitoring signal (55) is modified by considering in place of $\psi(t)$ its projection on $\partial\Omega_1$ along the radial direction. The overall scheme is detailed in the sidebar "Single Estimator-based Switching Controller". A remarkable feature of the proposed monitoring signal is that, given $\psi(t)$, the calculation of $\pi_i(t)$ requires no extra dynamics. Consequently, the complexity of the supervisor is not influenced by the size of the family of candidate controllers, hence the method can be easily extended to encompass multi-frequency disturbance. Similarly to the multi-model adaptive controller, the hysteresis-based logic rules out the possibility of Zeno behavior for the switching signal. The switching is guaranteed to stop in finite time, yielding a stabilizing controller that provides asymptotic regulation of the output $y(t)$.

EXPERIMENTAL STUDY

Adaptive feedforward and internal model-based techniques have found widespread application to the problem of rejecting acoustically generated noise, a setup that is commonly known under the moniker *active noise control* (ANC) [2]. A benchmark problem in this regard is the rejection of periodic disturbance in an instrumented acoustic duct [17], [54]–[56], where a disturbance signal is produced by a signal generator, amplified and transmitted to a closed or open chamber by a "noise loudspeaker". A control signal, generated by a feedback control algorithm, is sent to an "anti-noise loudspeaker," placed in the duct at a

Auxiliary Estimator-based Switching Controller

The architecture of the Single Estimator-based Switching Controller presented in [53] is comprised of three modules: A switching controller, an auxiliary estimator, and a hysteresis-based switching logic. Compared to the previously introduced multiple-model adaptive controller which maintains several parallel estimators, this approach significantly reduces computational complexity by employing only a single auxiliary estimator. The selection among candidate parameter values is then made using a simple distance-based criterion.

Switching Controller

Let $\sigma(\cdot) : \mathbb{R}_{\geq 0} \to \mathcal{I} = \{1, 2, \ldots, N\}$ be a piecewise constant switching signal, generated by a supervisor. The single observer-based switching controller (with piecewise continuous output)

$$\begin{aligned} \dot{\hat{\zeta}}_o(t) &= S\hat{\zeta}_o(t) + \hat{\vartheta}_{\sigma(t)} u_a(t) - \alpha \Gamma^\top (\hat{y}_a(t) - y(t)) \\ y_a(t) &= \Gamma \hat{\zeta}_o(t) \\ u_a^{\sigma(t)}(t) &= -\varepsilon \hat{\vartheta}_{\sigma(t)}^\top \hat{\zeta}_o(t), \end{aligned} \tag{S1}$$

is employed, where $\alpha > 0$ and $\varepsilon > 0$ are gains to be selected. The current value $\sigma(t) \in \mathcal{I}$ of the switching signal determines the output of the observer-based controller (S1) that drives the internal model unit

$$\begin{aligned} \dot{\eta}(t) &= S\eta(t) + \Gamma^\top u_a^{\sigma(t)}(t) \\ u(t) &= \Gamma \eta(t). \end{aligned}$$

Auxiliary Estimator

In place of the three estimators running in parallel employed in the Multiple-Model Adaptive Controller, we utilize an auxiliary estimator $\psi(t)$, which guides the supervisor to find the most suitable candidate ϑ_i for $\hat{\vartheta}_{\sigma(t)}$. The unconstrained update law $\tau(t)$ for $\psi(t)$ is defined as

$$\begin{aligned} \tau(t) &= -\rho \xi(t) \left(\Gamma \hat{\zeta}_o(t) - y(t) - \tilde{\psi}(t)^\top \xi(t) \right), \\ \dot{\xi}(t) &= (S - \alpha \Gamma^\top \Gamma)^\top \xi(t) + \Gamma^\top u_a^{\sigma(t)}(t), \; \xi(0) = 0 \end{aligned} \tag{S2}$$

where $\xi(t)$ is the state of the filter generating the regressor, $\rho > 0$ is the adaptation gain, and $\tilde{\psi}(t)$ is defined as

$$\tilde{\psi}(t) = \hat{\vartheta}_{\sigma(t)} - \psi(t). \tag{S3}$$

The unconstrained update law $\tau(t)$ is then projected on Ω_2, the smallest closed ball containing Θ

$$\tau(t) = \text{Proj}_{\Omega_2}\{\tau(t)\}$$

where $\text{Proj}_{\Omega_2}\{\cdot\}$ is the standard projection on Ω_2. The current value $\sigma(t) \in \mathcal{I}$ of the switching signal determines the current selection of the constant parameter estimate

$$\hat{\vartheta}_{\sigma(t)} = \hat{\vartheta}_i, \quad i \in \mathcal{I}$$

that generates the estimation error (S3).

Hysteresis-based Switching Logic

Based on the auxiliary estimator $\psi(t)$, a hysteresis switching logic is designed as

$$\sigma(t) = \underset{\sigma(t^-), j}{\arg\min} \left\{ \pi_j(t), \pi_{\sigma(t^-)}(t) - h \right\}, \quad j \in \mathcal{I} \setminus \{\sigma(t^-)\}$$

where $h > 0$ is the hysteresis parameter that avoids infinitely fast switchings, and $\pi_i(t)$ is a performance functional defined as

$$\pi_i(t) := \begin{cases} \|\hat{\theta}_i - \psi(t)\| & \text{if } \|\psi\| \geq r_1 \\ \|\hat{\theta}_i - \psi'(t)\| & \text{otherwise} \end{cases}, \quad i \in \mathcal{I}. \tag{S4}$$

In (S4), $\psi'(t)$ denotes the projection of $\psi(t)$ on $\partial\Omega_1$ along its radial direction, where Ω_1 is the closed ball defined by

$$\Omega_1 = \text{clos}\{\Omega_2 \setminus \Theta\},$$

that is, the closed ball whose boundary defines the inner boundary of Θ. This modification of the performance index $\pi_i(t)$ is made to ensure that a viable candidate $\hat{\vartheta}_i$ that is sufficiently close to $\psi(t)$ exists in case $\psi(t) \in \Omega_1$. An example of operation of the switching logic is presented in Figure S1.

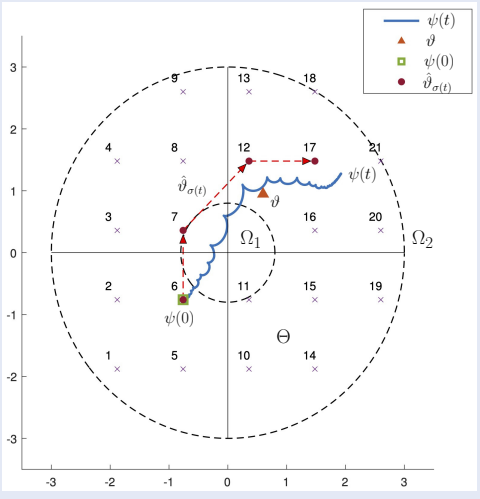

FIGURE S1 Example of parameter selection via auxiliary estimation. The supervisor selects the constant parameter estimate $\hat{\vartheta}_{\sigma(t)} = \hat{\vartheta}_i$ that is closest to the trajectory of the auxiliary continuous-time estimate $\psi(t)$. If $\psi(t)$ enters the ball Ω_1, the selection of $\hat{\vartheta}_{\sigma(t)}$ occurs at the boundary of Ω_1. Figure taken

different location than the noise loudspeaker. An "error microphone" detects the residual noise and feeds the output to be regulated to the control device for processing. The basic block diagram of an acoustic duct used as a test bench for ANC algorithms is shown in Figure 4. The diagram delineates two distinct pathways: the 'Primary Path' from the noise-generating loudspeaker to the error microphone, and the 'Secondary Path' from the anti-noise loudspeaker to the error microphone.

Experimental Setup

We designed an acoustic duct module with separate paths to manage noise and anti-noise signals. As seen in Figure 5, the acoustic duct is equipped with two error microphones, marked as microphone 1 and microphone 2, enabling path model variation by adjusting the microphone placement. The noise loudspeaker (disturbance speaker) generates the disturbance $d(t)$, while the anti-noise loudspeaker (control speaker) produces the anti-noise signal $u(t)$. The residual noise $y(t)$ is captured by the error microphones located near the pipe's open end. The disturbance and control

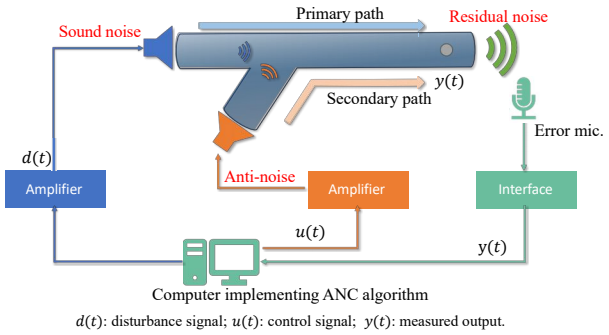

FIGURE 4 Block diagram of a typical acoustic duct for prototyping and testing ANC algorithms.

signals are generated by a computing device based on a cRIO-9049 NI 8-channel controller featuring a 1.60 GHz quad-core CPU with 4 GB DRAM and 16 GB storage for real-time control. Sampling is performed using an NI 9250 sound acquisition card with 2 channels and a synchronous

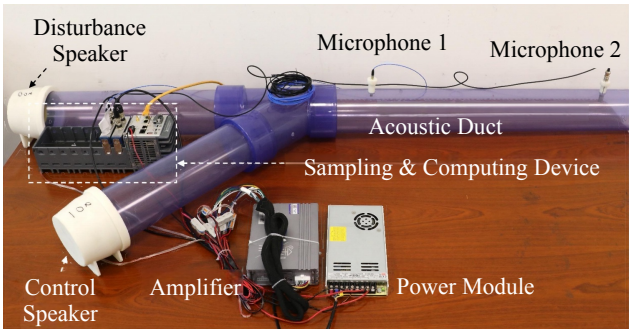

FIGURE 5 Experimental setup: Instrumented acoustic duct.

sampling rate of 102.4 kS/s. The transfer functions of the primary and secondary paths have not been identified. In all experiments, the sample time is set at 0.0002 s. The disturbance is selected as

$$d(t) = 0.75\sin(\omega t),$$

where $\omega = 200\pi$ rad/s.

Comparative Study

We conduct a comparative experimental study between the classic fixed-structure adaptive feedforward controller of [12], the switching internal model design of [46], the multiple-model adaptive design of [19], and the auxiliary estimator-based switching controller of [53]. The adopted nomenclature is reported in Table 1.

TABLE 1 Nomenclature

AFC	Adaptive Feedforward Control [12]
SW	Switching Internal Model [46]
MMA	Multiple-Model Adaptive Controller [19]
AUX	Auxiliary Estimator-based Switching Controller [53]

The parameters G_i, $i = 1,\ldots,4$, of the switching controller SW are labeled as in (30). The parameter set Θ is selected as in (35), with $r_1 = 0.2$ and $r_2 = 2$. The three independent parameter estimates $\hat{\vartheta}^i(t)$, $i = 1,2,3$, of the multiple model adaptive controller MMA are initialized

respectively as

$$\hat{\vartheta}^1(0) = \begin{pmatrix} -1 \\ 1 \end{pmatrix}, \quad \hat{\vartheta}^2(0) = \begin{pmatrix} 1 \\ 1 \end{pmatrix}, \quad \hat{\vartheta}^3(0) = \begin{pmatrix} 0 \\ -1 \end{pmatrix}.$$

For the auxiliary estimator-based switching controller, we consider a set of $N = 100$ constant parameter estimates $\hat{\vartheta}_i$, $i = 1,\dots,N$, distributed over the set Θ. The auxiliary parameter estimate $\psi(t)$ is initialized at one of the constant estimates, $\psi(0) = \hat{\vartheta}_i$, $i \in \{1,\dots,N\}$. For the switching-based controllers (SW, MMA, AUX), the switching mechanism is initialized according to two different case studies, which are described below. For both case studies, the initial value $\sigma(0)$ of the switching signal is reported in Table 2, together with the final value $\sigma(\infty)$. Finally, the controller gains are shown in Table 3. Unless specified otherwise, the same values are used in both case studies.

TABLE 2 Switching Signal

Method	Case study 1		Case study 2	
	$\sigma(0)$	$\sigma(\infty)$	$\sigma(0)$	$\sigma(\infty)$
SW	3	3	2	4
MMA	3	3	1	3
AUX	95	95	43	83

TABLE 3 Controller Gains

AFC	$\varepsilon = 0.4$ (case 1) $\quad G = G_3$ (case 1)
SW	$\varepsilon = 1$
MMA	$\varepsilon = 5 \quad \rho = 0.6 \quad h = 0.5$
AUX	$\varepsilon = 5 \quad \rho = 30 \quad h = 0.02 \quad \alpha = 5 \quad N = 100$

Case Study 1: Initialization Near a Known Stabilizing Controller

The first case study considers a benign case where the controllers are initialized at (or near) a stabilizing controller. It has been verified experimentally that, for the family of adaptive feedforward controllers (29), either selection

$$G_3 = \begin{pmatrix} -1 \\ 0 \end{pmatrix} \quad \text{or} \quad G_4 = \begin{pmatrix} 0 \\ 1 \end{pmatrix}$$

yields a stabilizing controller for $\varepsilon > 0$ sufficiently small.

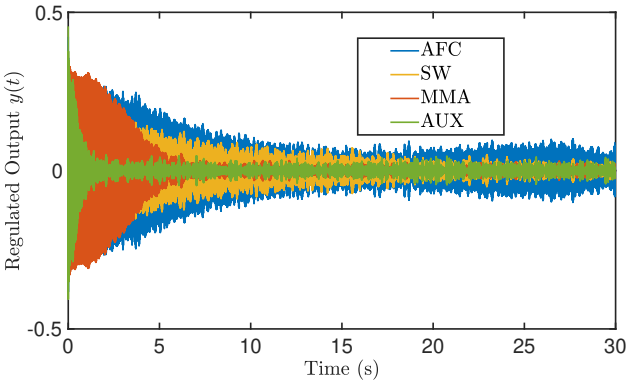

FIGURE 6 Comparative evaluation among the considered fixed-structure (AFC), switching (SW), and switching/adaptive controllers (MMA, AUX): Regulated output $y(t)$. Case study 1: Initialization near a known stabilizing solution.

This seems to suggest that the transfer function of the secondary path satisfies

$$\mathrm{Re}\{P(j\omega)\} < 0, \quad \mathrm{Im}\{P(j\omega)\} > 0$$

at the frequency of excitation. Accordingly, for the MMA and AUX controller, the true parameter vector ϑ appears to be located in either the subset Θ_3 or the subset Θ_1 of the cover $\bar{\Theta}$ (see Figure 3). Choosing G_3 for the adaptive feedforward algorithm and the initial value of the switching signal as in Table 2 ensures a stabilizing initial selection for all methods. As a matter of fact, the switching signal remains constant and equal to its initial value for all switching-based controllers. Figure 6 shows a comparison between the time histories of the regulated variable. It is noticed that the adaptive controllers MMA and AUX outperforms the switching and fixed-structure adaptive feedforward solutions, due also to a larger flexibility in the selection of the gain, which is especially limited for the AFC algorithm.

Case Study 2: Initialization Away from a Known Stabilizing Controller

The purpose of the second case study is to test the adaptation capabilities of the SW, MMA and AUX controllers. To this end, for each method, the switching signal is initialized at a different value than the one corresponding to the known stabilizing solution considered in the previous study. In particular, the initial values of the controller parameters $\hat{\vartheta}^{\sigma(0)}$, $\psi(0) = \hat{\vartheta}_{\sigma(0)}$ have been moved to a point in the parameter set located in the second quadrant of the cartesian plane while $G_{\sigma(0)} = G_2$. In this case, the switching mechanism for each controller reacts to a possibly unfavorable initialization, and ultimately selects a stabilizing internal model-based regulator. Figure 7 shows a comparison between the time histories of the regulated variable. Also in this case, it is noticed that the adaptive controllers MMA and AUX outperforms the switching controller SW in terms of speed of convergence and residual error. The evolution of the switching signal is shown in Figure 8. It is seen that different controllers than the initial ones are ultimately selected for the MMA and AUX method.

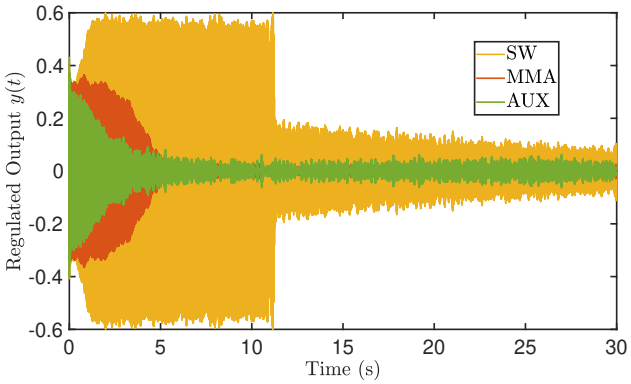

FIGURE 7 Comparative evaluation among the considered switching (SW) and switching/adaptive controllers (MMA, AUX): Regulated output $y(t)$. Case study 2: Initialization not at a known stabilizing solution.

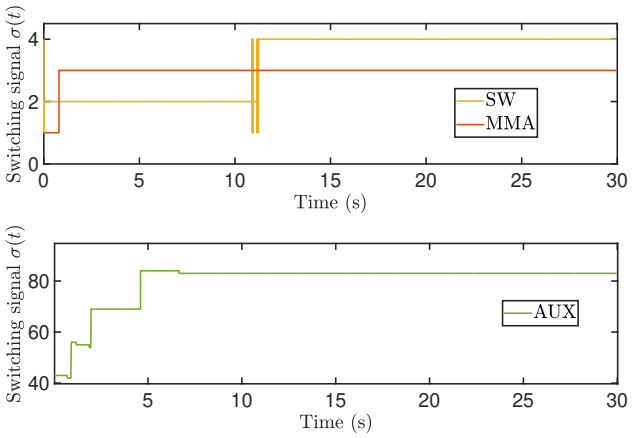

FIGURE 8 Comparative evaluation among the considered switching (SW) and switching/adaptive controllers (MMA, AUX): Switching signal $\sigma(t)$. Case study 2: Initialization not at a known stabilizing solution.

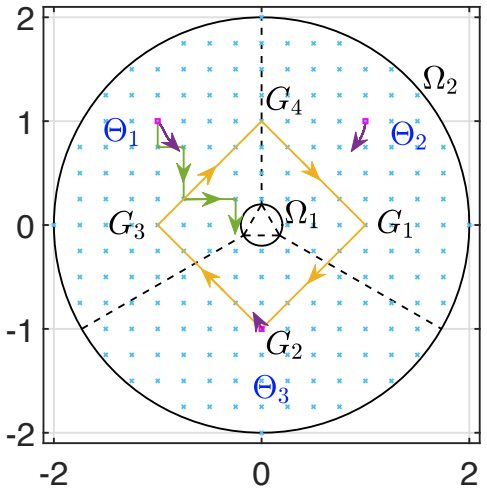

FIGURE 9 Comparative evaluation among the considered switching (SW) and switching/adaptive controllers (MMA, AUX): Parameter G_i for the switching controller (SW, shown in yellow); estimated parameters $\hat{\vartheta}^i(t)$, $i = 1, 2, 3$, for the multiple-model adaptive controller (MMA, shown in magenta), and piecewise constant estimated parameter $\hat{\vartheta}_{\sigma(t)}$ for the auxiliary estimator-based switching controller (AUX, shown in green). Case study 2: Initialization not at a known stabilizing solution.

Finally, Table 4 and Table 5 show comparative evaluations of various performance criteria across all considered methods in the two case studies. Specifically:

» The root mean-square error (RMSE) is computed using the **immse**$(\cdot)$ function in Matlab® with $y(t)$ in steady state.

» The convergence time is defined as the first time when $y(t)$ remains within 20% of the average steady-state amplitude.

» The attenuation in decibels (dB) using the formula

$$\text{Att} = 20\log_{10}\left(\frac{\text{Amplitude}_{\text{ANC}_{\text{on}}}}{\text{Amplitude}_{\text{ANC}_{\text{off}}}}\right).$$

Tables 4 and 5 also report the dynamic order of each controller. It is observed that, for the specific selection of the gains and initial conditions considered in these case studies, the MMA method appears to outperform the other adaptive and switching methods, apart from a better or similar performance in time of convergence provided by the AUX method. The advantages offered by the MMA, however, come at the price of higher dynamic order, which – as discussed – carries substantial difficulties when extended to multi-tone disturbances.

TABLE 4 Mean-squared Error and Convergence Time

Method	Order	RMSE		Convergence time (s)	
		Case 1	Case 2	Case 1	Case 2
AFC	2	0.0125	N/A	39.2666	N/A
SW	12	0.0139	0.0658	16.0126	21.0722
MMA	19	**0.0093**	**0.0094**	6.3364	**5.2924**
AUX	8	0.0127	0.0242	**1.4412**	5.3022

TABLE 5 Maximum Amplitude and Average Attenuation

Method	Order	Max Amplitude		Avg. Attenuation (dB)	
		Case 1	Case 2	Case 1	Case 2
AFC	2	0.4226	N/A	-18.9181	N/A
SW	12	0.3519	0.5994	-17.1120	-10.1475
MMA	19	**0.3283**	**0.3653**	**-21.6709**	**-22.0067**
AUX	8	0.4558	0.4293	-19.7762	-15.1909

FURTHER EXTENSIONS

» *Unknown Disturbance Frequencies:* In scenarios where the disturbance frequency is not known a priori, we have preliminarily explored a time-sharing switching strategy [30] that demonstrates the feasibility of disturbance rejection under large model uncertainties. However, this approach suffers from degraded transient performance due to cyclic switching. To overcome this limitation, we plan to incorporate frequency estimation modules into both the MMA and AUX frameworks. These modules will operate in parallel, enabling real-time estimation of disturbance frequencies and potentially improving both transient and steady-state performance.

» *Extension to MIMO Systems:* Extending the proposed approach to MIMO systems introduces challenges in designing certainty-equivalent control laws that account for multi-channel interactions while preserving stability and performance. As a preliminary step, our recent work [57] explores this idea in the context of multi-agent systems, which can be viewed as a structured form of MIMO systems. Future work will generalize these results to broader MIMO settings.

» *Nonlinear System:* An extension of AFC methodologies to converging nonlinear systems has been proposed in [58]. In future work, such extensions may be formalized and significantly expanded by leveraging contraction theory [59], [60] to adapt the internal model to nonlinear dynamics, particularly focusing on how higher-order harmonics can be attenuated and how the convergence properties of the system preserved in closed-loop.

TABLE 6 Comparison of Four Adaptive Feedforward Control Schemes.

Title	AFC	SW	MMA	AUX
Prior knowledge	Sign of θ	$\theta \neq 0$		
	Internally stable LTI plant; *No need for prior knowledge of plant dynamics*; Known disturbance frequency ω			
Main Idea	The sign of the frequency response is used to tune the parameter estimates.	A switching logic via SNE is employed for selecting the candidate internal model.	Three estimators are running in parallel with selection based on estimation error performance.	Viable constant estimates are selected using an auxiliary estimator and a distance-based performance index.
Controller	$u = \Gamma e^{St}\hat{w}_0$, $\dot{\hat{w}}_0 = -\varepsilon e^{-St}\Gamma^\top y$	$u = \Gamma\eta_{\sigma(t)}$, $\dot{\eta}_i = S\eta_i - \varepsilon G_i y \ i = 1,\ldots,4$	$u = \Gamma\eta$, $\dot{\eta} = S\eta + \Gamma^\top u_a$	
			$u_a = u_a^{\sigma(t)} = -\varepsilon\hat{\vartheta}^{\sigma(t)\top}\hat{\xi}_o^{\sigma(t)}$	$u_a = u_a^{\sigma(t)} = -\varepsilon\hat{\vartheta}_{\sigma(t)}^\top\hat{\xi}_o$
Pros	Simple implementation with relatively low dimensionality	SPR-like conditions are removed		
		Relatively low dimensionality	Improved transient performance; Robust to initial parameter estimates	Improved transient response; Minimal dimensionality (Dimension grows linearly with harmonics number)
Cons	SPR-like conditions needed; Relatively poor transient behavior	Relatively poor transient behavior	High dimensional growth with the number of harmonic components	Moderately sensitive to initial parameter estimates

CONCLUSIONS

We have provided an overview, we hope with a noticeable tutorial flavor, of classic results and recent developments in adaptive feedforward control design for stable, but uncertain, linear systems. We view this setup as yet another manifestation of the ubiquitous internal model principle of control theory, as well as an alternative to classic design methods. Throughout the paper, we have highlighted the connection with the output regulation problem within the internal model framework, and focused our attention to the problem of guaranteeing robustness of adaptive feedforward controllers to model uncertainty. We showed that, notwithstanding the fact that AFC schemes admit LTI realizations, adaptive and/or multi-model features are required in absence of specific (we believe restrictive) assumptions on the plant models.

AUTHOR INFORMATION

Yang Wang (wangyang4@shanghaitech.edu.cn) received her B.Eng. degree in Electrical and Electronic Engineering from Tongji University, Shanghai, China, in 2013, and the M.Sc. and Ph.D. degrees from Imperial College London, U.K., in 2014 and 2019, respectively. From 2014 to 2019, she held visiting scholar positions at the University of Cambridge, U.K., and Ohio State University, Ohio, USA. Since 2020, she has been an Assistant Professor at the School of Information Science and Technology, ShanghaiTech University, Shanghai, China. Her work has been supported by the Yangfan Program of STCSM, Shanghai. Her research interests lie at the intersection of nonlinear and adaptive control theory, with applications in fluidic systems, robotics, and automotive engineering.

Yizhou Gong (gongyzh2022@shanghaitech.edu.cn) received the B.S. degree in Automation from North China Electric Power University, China, in 2022. He is working toward the Ph.D. degree majoring in Electrical and Electronic Engineering at School of Information Science and Technology, ShanghaiTech University, Shanghai, China. His research interests include adaptive control, output regulation and observer design.

Chenyang Ji (jichy2024@shanghaitech.edu.cn) received the B.S. degree in Electronic Information Engineering from ShanghaiTech University, China, in 2024. He is working toward the Master degree majoring in Electrical and Electronic Engineering at School of Information Science and Technology, ShanghaiTech University, Shanghai, China. His research interests include active noise control and adaptive control.

Gilberto Pin (pingilbert@gmail.com) received the Laurea (M.Sc.) degree in Electrical Engineering (with honors) and the Ph.D. in Information Engineering from the University of Trieste, Italy, in 2005 and 2009, respectively. He has been an Automation Engineer at Danieli Automation S.p.A., Control Systems Engineer at the R&D Dept. of Electrolux Professional S.p.A., Senior Innovation Engineer at the Global Connectivity & Technology Center of Electrolux Italia S.p.A., and Global Model Based Design Manager at Electrolux Italia S.p.A. He has been Associate Professor of Automatic Control at Dept. of Information Engineering of the University of Padova, Italy. Presently, he is Algorithms & Embedded-AI manager at the Digital Technology Organization of Electrolux Italia S.p.A. He is co-recipient of the IFAC Best Application Paper Prize of the Journal of Process Control, Elsevier, for the three-year period 2011-2013 and of the Electrolux Invention Award in 2017. He has served as Associate Editor (AE) of the Conference Editorial Board (CEB) of the IEEE Control Systems Society and AE of the IEEE Trans. on Control Systems Technology.

Andrea Serrani (andrea.serrani@unibo.it) received the B.Eng. degree in Electrical Engineering in 1993, and the Ph.D. degree in 1997 from the University of Ancona, Italy. From 1994 to 1999, he was a Fulbright Fellow at Washington University in St. Louis, where he obtained the M.S. and D.Sc. degrees in Systems Science and Mathematics in 1996 and 2000, respectively. From 2002 to 2024, he was with the Department of Electrical and Computer Engineering at The Ohio State University. He is currently a Professor at the University of Bologna, Italy. He held visiting positions at the Universities of Bologna and Padua, Italy, and multiple summer faculty fellowships at AFRL. His research activity lies at the intersection of nonlinear, adaptive and geometric control theory with applications in aerospace and marine systems, fluidic systems, robotics and automotive engineering. Prof. Serrani was a Distinguished Lecturer of the IEEE CSS, and served as Editor-in-Chief of the IEEE Trans. on Control Systems Technology (2017-2024), and as an Associate Editor for the same journal, Automatica, and the Int. Journal of Robust and Nonlinear Control. He served as Program Chair for the 2019 ACC, and as General Co-chair for the 2022 IEEE CDC. He serves as VP-Publications and on the Board of Governors of the IEEE CSS.

Thomas Parisini (t.parisini@imperial.ac.uk) (Fellow, IEEE, IFAC) received the Ph.D. degree in electronic engineering and computer science from University of Genoa, Italy, in 1993. He was Associate Professor at Politecnico di Milano, Italy. He currently holds the Chair of Industrial Control, and is the Head of the Control and Power Research Group, Imperial College London, London, U.K. He also holds a Distinguished Professorship at Aalborg University, Denmark. Since 2001, he has been Danieli Endowed Chair of automation engineering with the University of Trieste, Italy, where from 2009 to 2012, he was Deputy Rector. He received the Knighthood of the Order of Merit of the Italian Republic awarded by the Italian President of the Republic in 2023. In 2018 he received the Honorary Doctorate from Aalborg University, Denmark, and in 2024 the IEEE CSS Transition to Practice Award. He was the 2021-2022 President of the IEEE Control Systems Society and the Editor-in-Chief of IEEE TRANSACTIONS ON CONTROL SYSTEMS TECHNOLOGY. He is the PI at Imperial of the H2020 EU flagship Teaming Project KIOS led by the University of Cyprus with an overall budget

of over 40 million Euros. He is a Member of IEEE TAB Periodicals Review and Advisory Committee.

REFERENCES

[1] I. D. Landau, T.-b. Airimitoaie, A. Castellanos-silva, and A. Constantinescu, *Adaptive and Robust Active Vibration Control*, ser. Advances in Industrial Control. Springer, 2017.

[2] S. M. Kuo and D. R. Morgan, "Active noise control: a tutorial review," *Proc. IEEE*, vol. 87, no. 6, pp. 943–973, 1999.

[3] T. Manayathara, T.-C. Tsao, and J. Bentsman, "Rejection of unknown periodic load disturbances in continuous steel casting process using learning repetitive control approach," *IEEE Transactions on Control Systems Technology*, vol. 4, no. 3, pp. 259–265, 1996.

[4] K. Chew and M. Tomizuka, "Digital control of repetitive errors in disk drive systems," *IEEE Control Systems Magazine*, vol. 10, no. 1, pp. 16–20, 1990.

[5] K. Ariyur and M. Krstic, "Feedback attenuation and adaptive cancellation of blade vortex interaction on a helicopter blade element," *IEEE Transactions on Control Systems Technology*, vol. 7, no. 5, pp. 596–605, 2002.

[6] D. Patt, D. Bernstein, J. Chandrasekar, P. Friedmann, and L. Liu, "Higher-harmonic-control algorithm for helicopter vibration reduction revisited," *Journal of Guidance, Control, and Dynamics*, vol. 28, no. 5, pp. 918–930, 2005.

[7] H. I. Basturk and M. Krstic, "Adaptive wave cancelation by acceleration feedback for ramp-connected air cushion-actuated surface effect ships," *Automatica*, vol. 49, no. 9, pp. 2591 – 2602, 2013.

[8] E. Davison, "The robust control of a servomechanism problem for linear time-invariant multivariable systems," *IEEE Transactions on Automatic Control*, vol. 21, no. 1, pp. 25–34, 1976.

[9] B. Francis, "The linear multivariable regulator problem," *SIAM Journal on Control and Optimization*, vol. 15, no. 3, pp. 486–505, 1977.

[10] B. Francis and W. Wonham, "The internal model principle of control theory," *Automatica*, vol. 12, no. 5, pp. 457–465, sep 1976.

[11] A. Isidori, *Lectures in feedback design for multivariable systems*. Springer, 2017.

[12] M. Bodson, A. Sacks, and P. Khosla, "Harmonic generation in adaptive feedforward cancellation schemes," *IEEE Transactions on Automatic Control*, vol. 39, no. 9, pp. 1939–1944, 1994.

[13] W. Messner and M. Bodson, "Design of adaptive feedforward algorithms using internal model equivalence," *International Journal of Adaptive Control and Signal Processing*, vol. 9, no. 2, pp. 199–212, 1995.

[14] B. Wu and M. Bodson, "Multi-channel active noise control for periodic sources—indirect approach," *Automatica*, vol. 40, no. 2, pp. 203–212, 2004.

[15] G. Pin, "A direct approach for the frequency-adaptive feedforward cancellation of harmonic disturbances," *IEEE Transactions on Signal Processing*, vol. 58, no. 7, pp. 3523–3530, 2010.

[16] S. Aranovskiy and L. B. Freidovich, "Adaptive compensation of disturbances formed as sums of sinusoidal signals with application to an active vibration control benchmark," *European Journal of Control*, vol. 19, no. 4, pp. 253–265, 2013.

[17] S. Pigg and M. Bodson, "Adaptive Algorithms for the Rejection of Sinusoidal Disturbances Acting on Unknown Plants," *IEEE Transactions on Control Systems Technology*, vol. 18, no. 4, pp. 822–836, 2010.

[18] R. Marino and P. Tomei, "Output Regulation for Unknown Stable Systems," *IEEE Transactions on Automatic Control*, vol. 60, no. 8, pp. 2213–2218, 2015.

[19] Y. Wang, G. Pin, A. Serrani, and T. Parisini, "Removing SPR-like conditions in adaptive feedforward control of uncertain systems," *IEEE Transactions on Automatic Control*, vol. 65, no. 6, pp. 2309–2324, 2020.

[20] K. S. Narendra and A. M. Annaswamy, *Stable adaptive systems*. Englewood Cliffs, NJ: Prentice Hall, 1989.

[21] P. Ioannou and J. Sun, *Robust Adaptive Control*. Upper Saddle River, NJ: Prentice Hall, 1996.

[22] J. Hale, *Ordinary Differential Equations*, ser. Dover Books on Mathematics Series. Dover Publications, 2009.

[23] P. Kokotovic, B. Riedle, and L. Praly, "On a stability criterion for continuous slow adaptation," *Systems & Control Letters*, vol. 6, no. 1, pp. 7–14, 1985.

[24] S. Sastry and M. Bodson, *Adaptive Control: Stability, Convergence, and Robustness*. Prentice-Hall, 1989.

[25] H. K. Khalil, *Nonlinear Systems*, 3rd ed. Upper Sddle River, NJ: Prentice Hall, 2002.

[26] A. Isidori, *Nonlinear Control System II*. Springer Verlag, 1999.

[27] L. Chen and J. W. Simpson-Porco, "Data-driven output regulation using single-gain tuning regulators," in *2023 62nd IEEE Conference on Decision and Control (CDC)*. IEEE, 2023, pp. 2903–2909.

[28] D. Astolfi, J. W. Simpson-Porco, and G. Scarciotti, "On the role of dual sylvester and invariance equations in systems and control," *IFAC-PapersOnLine*, vol. 58, no. 5, pp. 20–27, 2024.

[29] S. Fujii, J. P. Hespanha, and A. S. Morse, "Supervisory control of families of noise suppressing controllers," in *Proceedings of the 37th IEEE Conference on Decision and Control*, vol. 2, Tampa, FL, 1998, pp. 1641–1646.

[30] Y. Wang, A. Serrani, G. Pin, and T. Parisini, "Switching-based regulation of uncertain stable linear systems affected by an unknown harmonic disturbance," *IFAC-PapersOnLine*, vol. 52, no. 16, pp. 604–609, 2019, 11th IFAC Symposium on Nonlinear Control Systems NOLCOS 2019.

[31] Y. Wang, G. Pin, A. Serrani, and T. Parisini, "Switching-based rejection of an unknown harmonic disturbance in uncertain stable linear systems under measurement noise," in *Proceedings of the 2019 American Control Conference*, Philadelphia, PA, 2019, pp. 3020–3025.

[32] R. Marino and P. Tomei, "Hybrid adaptive multi-sinusoidal disturbance cancellation," *IEEE Transactions on Automatic Control*, vol. 62, no. 8, pp. 4023–

4030, 2017.

[33] M. Bin, L. Marconi, and A. R. Teel, "Adaptive output regulation for linear systems via discrete-time identifiers," *Automatica*, vol. 105, pp. 422–432, 2019.

[34] M. Bin, P. Bernard, and L. Marconi, "Approximate nonlinear regulation via identification-based adaptive internal models," *IEEE Transactions on Automatic Control*, vol. 66, no. 8, pp. 3534–3549, 2021.

[35] M. Bodson and S. Douglas, "Adaptive algorithms for the rejection of sinusoidal disturbances with unknown frequency," *Automatica*, no. 12, pp. 2213–2221, 1997.

[36] V. Nikiforov, "Adaptive non-linear tracking with complete compensation of unknown disturbances," *European Journal of Control*, vol. 4, no. 2, pp. 132–139, 1998.

[37] A. Serrani, A. Isidori, and L. Marconi, "Semi-global nonlinear output regulation with adaptive internal model," *IEEE Transactions on Automatic Control*, vol. 46, no. 8, pp. 1178–1194, Aug 2001.

[38] R. Marino and P. Tomei, "Output regulation for linear systems via adaptive internal model," *IEEE Transactions on Automatic Control*, vol. 48, no. 12, pp. 2199–2202, 2003.

[39] L. Brown and Q. Zhang, "Periodic disturbance cancellation with uncertain frequency," *Automatica*, vol. 40, no. 4, pp. 631–637, 2004.

[40] F. Ben-Amara, P. Kabamba, and A. Ulsoy, "Adaptive sinusoidal disturbance rejection in linear discrete-time systems. I. Theory–II. Experiments," *Transactions of the ASME. Journal of Dynamic Systems, Measurement and Control*, vol. 121, no. 4, pp. 648–659, 1999.

[41] Y. Wang, G. Pin, A. Serrani, and T. Parisini, "Switching-based sinusoidal disturbance rejection for uncertain stable linear systems," in *2018 American Control Conference*, Milwaukee, WI, 2018.

[42] A. S. Morse, "Control using logic-based switching," in *Trends in Control. A European Perspective*, A. Isidori, Ed. Springer Verlag, 1995, pp. 69–113.

[43] J. P. Hespanha, D. Liberzon, and A. Morse, "Hysteresis-based switching algorithms for supervisory control of uncertain systems," *Automatica*, vol. 39, no. 2, pp. 263 – 272, 2003.

[44] M. Cao and A. S. Morse, "Dwell-time switching," *Systems and Control Letters*, vol. 59, no. 1, pp. 57–65, 2010.

[45] A. S. Morse, "Lecture notes on logically switched dynamical systems," in *Nonlinear and Optimal Control Theory: Lectures given at the CIME Summer School held in Cetraro, Italy*, P. Nistri and G. Stefani, Eds. Springer Verlag, 2008, pp. 61–161.

[46] Y. Wang, G. Pin, A. Serrani, and T. Parisini, "Switching-based rejection of multi-sinusoidal disturbance in uncertain stable linear systems under measurement noise," in *Proceedings of the 58th IEEE Conference on Decision and Control*, Nice, France, 2019, pp. 6112–6117.

[47] M. A. Müller and D. Liberzon, "Input/output-to-state stability and state-norm estimators for switched nonlinear systems," *Automatica*, vol. 48, no. 9, pp. 2029 – 2039, 2012.

[48] R. Middleton, G. Goodwin, D. Hill, and D. Mayne, "Design issues in adaptive control," *IEEE Transactions on Automatic Control*, vol. 33, no. 1, pp. 50–58, 1988.

[49] A. S. Morse, D. Q. Mayne, and G. C. Goodwin, "Applications of hysteresis switching in parameter adaptive control," *IEEE Transaction on Automation and Control*, vol. 37, no. 9, pp. 1343–1354, 1992.

[50] K. Narendra and J. Balakrishnan, "Adaptive control using multiple models," *IEEE Transactions on Automatic Control*, vol. 42, no. 2, pp. 171–187, 1997.

[51] B. D. O. Anderson, T. S. Brinsmead, F. De Bruyne, J. Hespanha, D. Liberzon, and A. S. Morse, "Multiple model adaptive control. Part 1: Finite controller coverings," *International Journal of Robust and Nonlinear Control*, vol. 10, no. 11-12, pp. 909–929, 2000.

[52] J. Hespanha, D. Liberzon, S. A. Morse, B. D. O. Anderson, T. S. Brinsmead, and F. De Bruyne, "Multiple model adaptive control. Part 2: Switching," *International Journal of Robust and Nonlinear Control*, vol. 11, no. 5, pp. 479–496, 2001.

[53] G. He, Y. Wang, G. Pin, A. Serrani, and T. Parisini, "Switching-based adaptive output regulation for uncertain systems affected by a periodic disturbance," in *2022 American Control Conference*, Atlanta, GA, 2022, pp. 5030–5036.

[54] H. R. Pota and A. G. Kelkar, "Modeling and control of acoustic ducts," *Journal of Vibration and Acoustics*, vol. 123, no. 1, pp. 2–10, 2000.

[55] M. Bodson, J. Jensen, and S. Douglas, "Active noise control for periodic disturbances," *IEEE Transactions on Control Systems Technology*, vol. 9, no. 1, pp. 200–205, 2001.

[56] J. Chandrasekar, L. Liu, D. Patt, P. Friedmann, and D. Bernstein, "Adaptive Harmonic Steady-State Control for Disturbance Rejection," *IEEE Transactions on Control Systems Technology*, vol. 14, no. 6, pp. 993–1007, 2006.

[57] Y. Gong and Y. Wang, "A novel plug-and-play cooperative disturbance compensator for heterogeneous uncertain linear multi-agent systems," *IEEE Control Systems Letters*, vol. 8, pp. 2811–2816, 2024.

[58] S. Messineo and A. Serrani, "Adaptive feedforward disturbance rejection in nonlinear systems," *Systems & Control Letters*, vol. 58, no. 8, pp. 576–583, 2009.

[59] A. Pavlov and L. Marconi, "Incremental passivity and output regulation," *Systems & Control Letters*, vol. 57, no. 5, pp. 400–409, 2008.

[60] D. Astolfi, L. Praly, and L. Marconi, "Harmonic internal models for structurally robust periodic output regulation," *Systems & Control Letters*, vol. 161, p. 105154, 2022.